The EMBO Journal (2013) 32, 2039–2055
www.embojournal.org

TRANSPARENT PROCESS

THE EMBO JOURNAL

Ral mediates activity-dependent growth of postsynaptic membranes *via* recruitment of the exocyst

Rita O Teodoro[1,2,*], Gulçin Pekkurnaz[1,2], Abdullah Nasser[1,2], Misao E Higashi-Kovtun[1,2], Maria Balakireva[3], Ian G McLachlan[1,2], Jacques Camonis[3] and Thomas L Schwarz[1,2,*]

[1]The F.M. Kirby Neurobiology Center, Department of Neurology, Boston Children's Hospital, Boston, MA, USA, [2]Department of Neurobiology, Harvard Medical School, Boston, MA, USA and [3]Institut Curie, Inserm U830, Paris, France

Remodelling neuronal connections by synaptic activity requires membrane trafficking. We present evidence for a signalling pathway by which synaptic activity and its consequent Ca^{2+} influx activate the small GTPase Ral and thereby recruit exocyst proteins to postsynaptic zones. In accord with the ability of the exocyst to direct delivery of post-Golgi vesicles, constitutively active Ral expressed in *Drosophila* muscle causes the exocyst to be concentrated in the region surrounding synaptic boutons and consequently enlarges the membrane folds of the postsynaptic plasma membrane (the subsynaptic reticulum, SSR). SSR growth requires Ral and the exocyst component Sec5 and Ral-induced enlargement of these membrane folds does not occur in *sec5*$^{-/-}$ muscles. Chronic changes in synaptic activity influence the plastic growth of this membrane in a manner consistent with activity-dependent activation of Ral. Thus, Ral regulation of the exocyst represents a control point for postsynaptic plasticity. This pathway may also function in mammals as expression of activated RalA in hippocampal neurons increases dendritic spine density in an exocyst-dependent manner and increases Sec5 in spines.

The EMBO Journal (2013) **32,** 2039–2055. doi:10.1038/emboj.2013.147; Published online 28 June 2013
Subject Categories: membranes & transport; neuroscience
Keywords: dendritic spine; *Drosophila* neuromuscular junction; membrane trafficking; subsynaptic reticulum (SSR); synaptic activity

*Corresponding authors. RO Teodoro, Department of Neuroscience, Boston Children's Hospital/Harvard Medical School, 3 Blackfan Circle, CLS 12-120, Boston, MA 02115, USA. Tel.: +1 617 919 2264; Fax: +1 617 919 2771; E-mail: rita.o.teodoro@gmail.com
or TL Schwarz, The F.M. Kirby Neurobiology Center, Boston Children's Hospital and Department of Neurobiology, Harvard Medical School, 3 Blackfan Street, CLS 12-130, Boston, MA 02115, USA.
Tel.: +1 617 919 2219; Fax: +1 617 919 2771;
E-mail: thomas.schwarz@childrens.harvard.edu

Received: 28 November 2012; accepted: 28 May 2013; published online: 28 June 2013

Introduction

Cell morphology determines many functional aspects of a neuronal network and achieving the correct morphology requires precisely regulated protein and membrane traffic to specific domains. The primary shape of a neuron is established during axon and dendrite outgrowth and synapse formation, but is subjected to subsequent modifications by physiological events. In response to changes in synaptic activity, neurons can alter both pre- and postsynaptic elements of the synapse, including the number, size, and shape of dendritic spines (Kennedy and Ehlers, 2006; Alvarez and Sabatini, 2007; Bourne and Harris, 2007; Hanus and Ehlers, 2008; Newpher and Ehlers, 2009; Kasai *et al*, 2010). Because of the importance of these morphological events, membrane trafficking is emerging as a key aspect of neuronal development and plasticity. Membrane addition is critical for permitting neurite outgrowth and branching (Steiner *et al*, 2002; Lalli and Hall, 2005) and both membrane addition and membrane internalization are required for the growth and retraction of spines (Holtmaat and Svoboda, 2009; Newpher and Ehlers, 2009; Kelly *et al*, 2011). Exocytic trafficking from recycling compartments contributes to dendritic spine growth in response to activity (Park *et al*, 2006; Kennedy *et al*, 2010), but the main source of membrane responsible for this growth and the signals that control membrane addition remain elusive. Moreover, the localization of these events to precise regions of the neuronal surface is necessary to establish or modify appropriately synaptic connectivity.

The exocyst is a protein complex that can govern the polarized cell-surface delivery of membrane and membrane proteins (Munson and Novick, 2006; Wu *et al*, 2008; He and Guo, 2009; Jin *et al*, 2011). The exocyst comprises eight proteins conserved from yeast to man and, although not required for the exocytosis of synaptic vesicles (Murthy *et al*, 2003), the exocyst may be important in other aspects of synapse growth and plasticity through its involvement in and regulation of the tethering, docking, and fusion of post-Golgi vesicles with the plasma membrane. It is required for neurite outgrowth and the addition of neuronal membrane proteins, including the insertion of glutamate receptors, and the maturation of photoreceptors (Brymora *et al*, 2001; Vega and Hsu, 2001; Murthy *et al*, 2003; Sans *et al*, 2003; Beronja *et al*, 2005; Liebl *et al*, 2005; Mehta *et al*, 2005; Gerges *et al*, 2006). The distribution of the exocyst within a cell can be highly dynamic, consistent with its role in directing membrane fusion to specific domains (Boyd *et al*, 2004; Beronja *et al*, 2005; Mehta *et al*, 2005; Zhang *et al*, 2008; Murthy *et al*, 2010).

Recent studies have examined the manner in which the exocyst is assembled and localized and have identified regulatory interactions of exocyst proteins with several small GTPases (Lipschutz and Mostov, 2002; Wu *et al*, 2008), including the two mammalian Ral isoforms, RalA and RalB.

Like the exocyst, Ral is expressed in the nervous system (Ngsee *et al*, 1991; Huber *et al*, 1994; Peng *et al*, 2004; Han *et al*, 2009). RalA binds directly to the exocyst members Sec5 and Exo84 and this interaction is thought to promote complex assembly, vesicle exocytosis, and membrane addition (Moskalenko *et al*, 2002, 2003; Sugihara *et al*, 2002; Fukai *et al*, 2003; Mott *et al*, 2003; Wang *et al*, 2004; Jin *et al*, 2005; Hase *et al*, 2009). Ral can be activated either by Ras indirectly via a Ral-GEF (Guanine nucleotide Exchange Factor) or by Ca^{2+}/calmodulin binding (Hofer *et al*, 1994, 1998; Kikuchi *et al*, 1994; Wolthuis *et al*, 1998; Wang and Roufogalis, 1999; Wolthuis and Bos, 1999; Harvey *et al*, 2008), and it is inactivated by PKC phosphorylation of the effector Sec5 (Chen *et al*, 2011). Both Ca^{2+} and Ras can regulate synaptic development and plasticity (Tada and Sheng, 2006; Alvarez and Sabatini, 2007; Harvey *et al*, 2008). We therefore took advantage of the evolutionary conservation of the exocyst and Ral pathways in *Drosophila*, to ask whether a Ral/exocyst pathway also plays a role in modifying synapses.

The *Drosophila* neuromuscular junction (NMJ) is a glutamatergic synapse that has proven to be a good model system to study synaptic development and plasticity (Collins and DiAntonio, 2007). Plastic changes to its morphology include a 10-fold increase in synaptic boutons from the first- to the third-larval instars and activity-dependent changes in bouton number and shape. A prominent feature of this synapse, though one that has received less attention, is the elaborate set of postsynaptic folds of the plasma membrane called the subsynaptic reticulum (SSR). This structure develops during the second half of larval life and is also present at the NMJs of other arthropods (Jahromi and Atwood, 1974; Rheuben, 1985; Feeney *et al*, 1998). Glutamate receptors reside in the muscle membrane immediately across the synaptic cleft from presynaptic active zones. The folds of the SSR underlie these receptor fields and surround the presynaptic boutons. The SSR contains scaffolding proteins and cytoskeletal specializations (Rheuben *et al*, 1999; Ataman *et al*, 2006), but the significance of the SSR is poorly understood. The time course of its development suggests that it may be an adaptation that allows receptor-activated currents to depolarize the low input resistance of these large muscle fibres. Its architecture, like that of mammalian dendritic spines, likely allows signal compartmentalization and the generation of postsynaptic micro-domains that can sculpt synaptic responses.

We here report that the SSR is a plastic structure whose size depends on synaptic activity. Synaptically driven Ca^{2+} influx activates synaptically localized Ral and, by recruiting the exocyst complex to the postsynapse, causes the postsynaptic membranes to grow. Our initial studies in mammalian neurons further suggest conservation of Ral/exocyst-induced postsynaptic growth as a form of plasticity.

Results

Postsynaptic activated Ral recruits Sec5 to the synapse

To examine Ral regulation of the exocyst at the NMJ, we expressed previously characterized wild-type, constitutively active, and inactive transgenes of Ral (Ral^{WT}, Ral^{CA}, and Ral^{inact}) in the larval body wall by using a muscle-specific driver, MHC-Gal4. The Ral^{CA} and Ral^{inact} transgenes contain mutations (G20V and S25N) that render Ral in the active GTP-bound or inactive GDP-bound state (Mirey *et al*, 2003). A newly developed antibody to *Drosophila* Ral demonstrated that both Ral^{CA} and Ral^{inact} became highly concentrated at the NMJs of third-instar larvae (Figure 1A and B). This antibody recognized a band corresponding to endogenous Ral and absent from *ral* mutant larvae on a western blot (Supplementary Figure S1A), but was not adequate to detect endogenous Ral by immunocytochemistry. Because Ral directly binds to Sec5 and Sec5 is a core component of the exocyst, we examined Sec5 localization at these synapses. As shown in Figure 1C, in wild-type larvae, Sec5 immunoreactivity was observed in both the nerve and muscle and only modestly enriched around the NMJ. When Ral^{CA} was expressed in the muscles, we observed a significant recruitment of Sec5 towards the area around the synaptic boutons (Figure 1D). The phenomenon occurred at type I boutons throughout the larva but was analysed selectively at the well-characterized synapses on muscles 6 and 7 in segments A2 and A3. In contrast to the effect of Ral^{CA}, Ral^{inact} expression produced no detectable change in Sec5 distribution (Figure 1E). Expression of Ral wild-type (Ral^{WT}) in the muscle showed a Ral^{CA} phenotype, though less pronounced, likely due to partial activation of Ral^{WT} (Figure 1H). Ral^{CA} was also expressed in motor neurons via the driver OK6-Gal4, and Sec5 distribution at the NMJ was unchanged (Figure 1F). Nor did muscle expression of a constitutively active transgene of Rab11 ($Rab11^{CA}$), a small GTPase that has been shown to interact with the exocyst complex protein Sec15 (Wu *et al*, 2005), change Sec5 distribution (Figure 1G). Significant enrichment of Sec5 to the synaptic region occurred only when Ral^{CA} or Ral^{WT} was expressed in the muscle (Figure 1H). When we examined other exocyst components, Sec15 immunoreactivity (Figure 1I–J) and the epitope-tagged transgenes Sec3-HA and Sec8-HA (Supplementary Figure S1B–E) also became concentrated in the vicinity of the boutons in muscles expressing Ral^{CA}. Thus, activated Ral appears to recruit exocyst complexes and not just Sec5 to the NMJ. Because both Ral^{CA} and Ral^{inact} (Figure 1A and B) localize to the NMJ, but only active Ral can recruit Sec5 to the NMJ (Figure 1D and E), it indicates that the synaptic localization of Ral is independent of its nucleotide state, but the recruitment of the exocyst occurs only in the GTP-bound state.

Consequences of postsynaptic Ral^{CA} expression on synaptic proteins

To understand the relevance of the Ral-mediated Sec5 recruitment to the NMJ, we recorded from muscle 6 in third-instar larvae, and examined the distribution of known components of that synapse. Only minor electrophysiological differences were observed between muscles expressing Ral^{CA} and controls: the amplitude of evoked excitatory postsynaptic potentials (EPSPs) was unchanged and the spontaneous miniature EPSP (mEPSP) amplitude and frequency were mildly reduced (Supplementary Figure S2A). The presence of normal EPSPs despite smaller mEPSPs can likely be attributed to a homeostatic increase in quantal content (Davis and Bezprozvanny, 2001; Heckscher *et al*, 2007). The number of synaptic boutons also appeared unchanged by Ral^{CA} expression in the muscle (control $= 131 \pm 6$ versus muscle $Ral^{CA} = 133 \pm 5$) but immunocytochemical characteri-

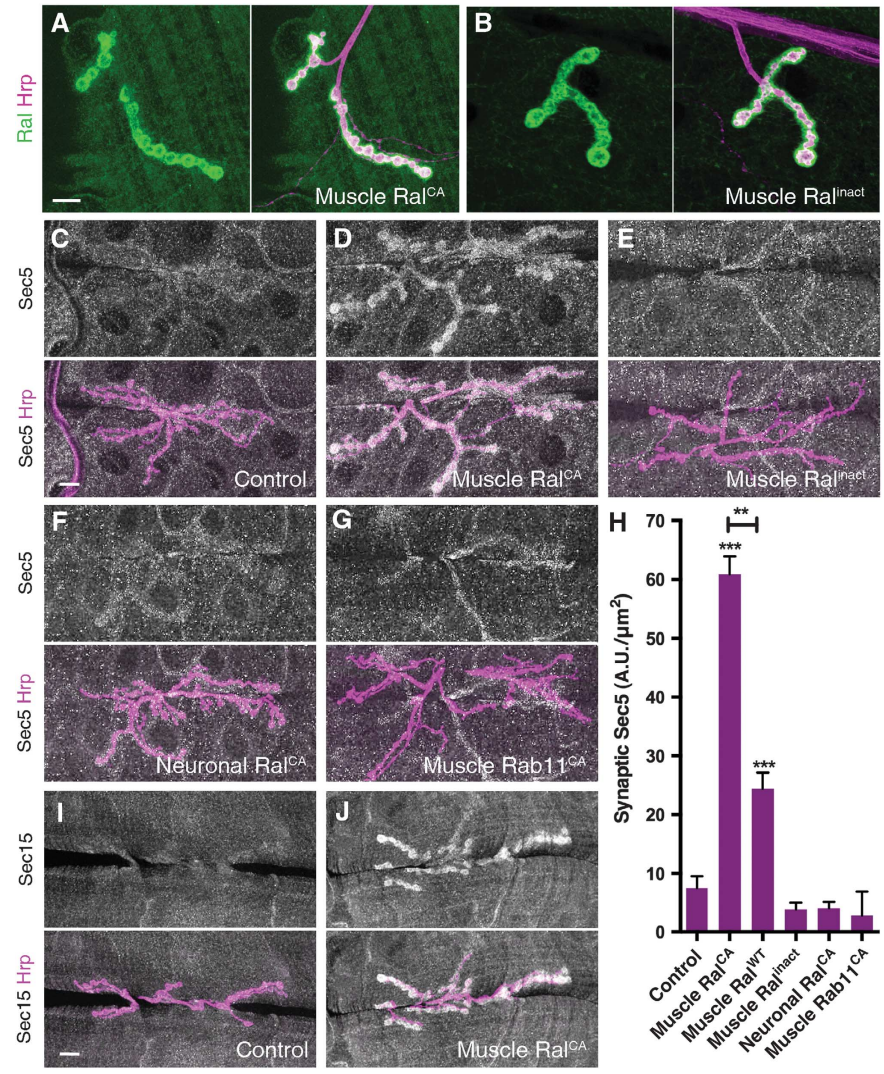

Figure 1 Activation of RalA in muscle recruits Sec5 and Sec15 to the NMJ. (**A**, **B**) Expressed Ral localizes to NMJs labelled with anti-Ral (green) and the neuronal marker anti-HRP (magenta) regardless of the nucleotide-bound state of Ral. (**A**) Muscle expression of Ral^{CA} (MHC-Gal4/UAS-Ral^{CA}) and (**B**) muscle expression of Ral^{inact} (MHC-Gal4/UAS-Ral^{inact}). (**C–G**) NMJs labelled with anti-Sec5 (grey) and the neuronal marker anti-HRP (magenta). Sec5 accumulates in the vicinity of the synapse when Ral^{CA} is expressed in the muscle but not in neurons. (**C**) Control (MHC-Gal4/+), (**D**) muscle expression of Ral^{CA} (MHC-Gal4/UAS-Ral^{CA}), (**E**) muscle expression of Ral^{inact} (MHC-Gal4/UAS-Ral^{inact}), (**F**) neuronal expression of Ral^{CA} (OK6-Gal4/UAS-Ral^{CA}), and (**G**) muscle expression of Rab11^{CA} (MHC-Gal4/UAS-Rab11^{CA}-YFP). (**H**) Quantification of synaptic Sec5 in the genotypes shown in (**C–G**), and in muscle expression of Ral^{WT} (MHC-Gal4/UAS-Ral^{WT}). The mean ± s.e.m. is shown, $***P<0.0001$, $**P<0.01$. (**I**, **J**) Muscle expression of Ral^{CA} also recruits Sec15 (grey) to the vicinity of the synapse (anti-Hrp; magenta). (**I**) Control (MHC-Gal4/+) and (**J**) muscle Ral^{CA} (MHC-Gal4/UAS-Ral^{CA}). For all images, scale bar is 10 μm.

zation of synaptic proteins indicated shifts in synaptic composition. The presynaptic markers Bruchpilot (Brp) and Synaptotagmin I (SytI), which reside in active zones and synaptic vesicles, were similar in pattern and intensity in control and Ral^{CA}-expressing muscles (Figure 2A). To characterize postsynaptic composition, we examined the distribution and quantified the intensity of immunolabelling for the glutamate receptor subunits GluRIIA and GluRIIB, the scaffolding protein Discs Large (Dlg), the cell-adhesion molecule Fasciclin-II, the postsynaptic signalling proteins Par-1, Pak, and Pix, and the structural proteins α-Spectrin and Syndapin-1. Many of these components were not significantly altered by the expression of Ral^{CA} (Figure 2A). There were, however, some differences: GluRIIB receptor and Par-1 levels were increased by 22 and 35%, respectively, and Dlg was reduced by 20% (Figure 2A; Supplementary Figure S2B and C). The greatest change, however, was observed in levels of the F-bar protein, Syndapin-1, which increased by ∼70% of control levels (Figure 2A–C).

Syndapin is a peripheral membrane protein located in the SSR and its F-bar domain may contribute to the folding and tubulation of this postsynaptic membrane network (Kumar *et al*, 2009; Wang *et al*, 2009; Rao *et al*, 2010). Overexpression of Syndapin promotes the growth of the SSR (Kumar *et al*, 2009), and the increase in Syndapin at the NMJ therefore suggested that exocyst recruitment by Ral might have caused SSR growth.

Postsynaptic expression of Ral^{CA} promotes SSR expansion

To examine the involvement of Ral and the exocyst in SSR growth, we performed transmission electron microscopy

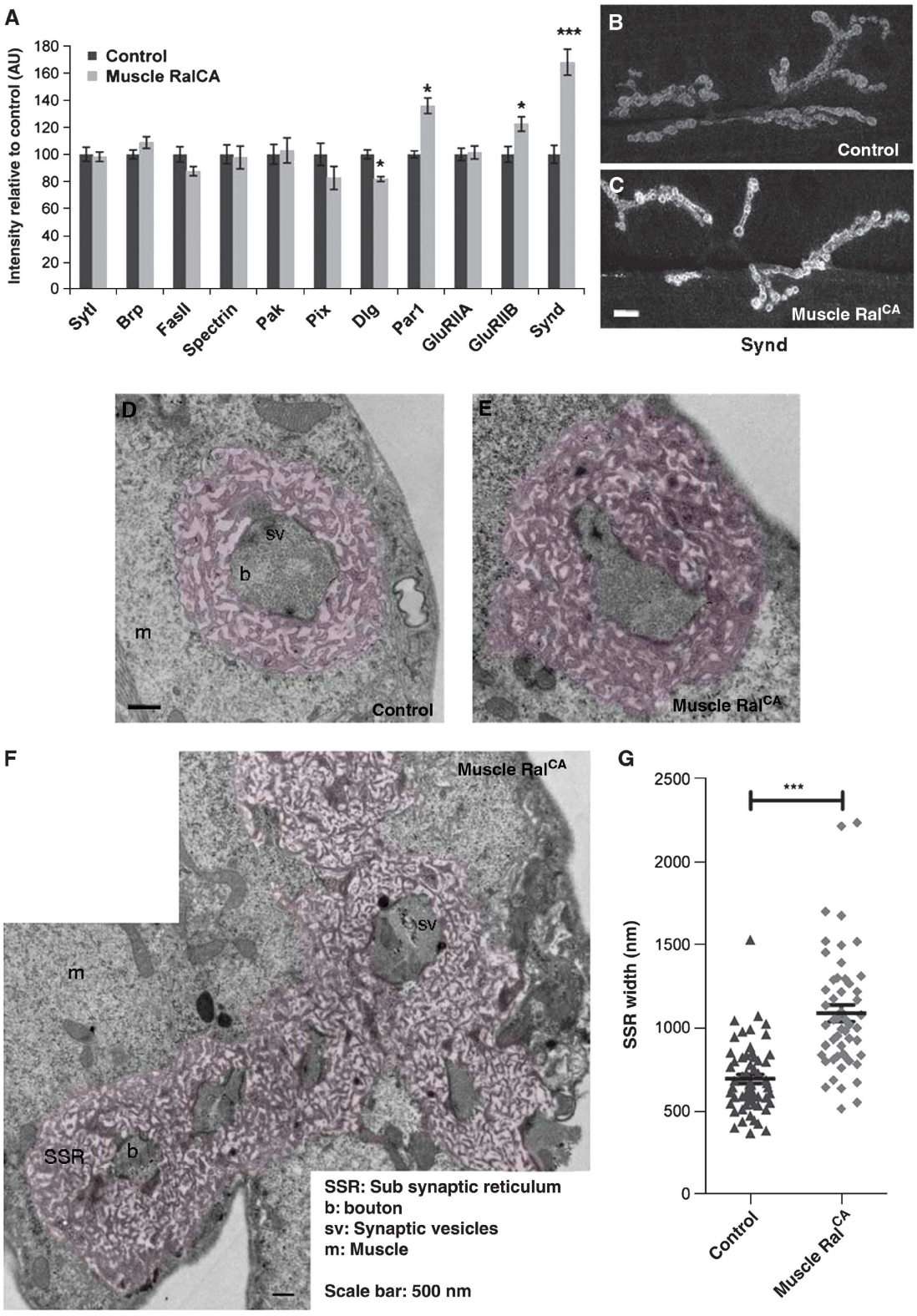

Figure 2 Ral^{CA} expression increases Syndapin levels and enlarges the subsynaptic reticulum (SSR) in third-instar muscles. (**A**) The effect of expressing Ral^{CA} in larval muscles on the fluorescent intensity at synapses of the indicated proteins. Synaptotagmin I (SytI), Bruchpilot (Brp), Fasciclin II (FasII), Discs large (Dlg), Glutamate Receptor type II subunits A and B (GluRIIA and GluRIIB), and Syndapin (Synd). Fluorescence intensity (mean ± s.e.m.) was normalized to that in control larvae, $^{*}P<0.05$ and $^{***}P<0.001$. (**B** and **C**) Representative examples of Syndapin immunolabelling at a control NMJ (MHC/+) and NMJ-expressing muscle Ral^{CA} (MHC-Gal4/UAS-Ral^{CA}). Scale bar is 10 μm. (**D–F**) Electron micrographs of third-instar larval NMJs from the indicated genotypes. Expression of Ral^{CA} caused a larger SSR and at times, as in **F**, the SSR formed a continuous zone between adjacent boutons rather than the discrete halo around each bouton that is typical of control muscles. Scale bar is 500 nm in each. (**G**) Quantification of SSR width. Each point represents the SSR width around an individual type Ib bouton; at least six animals were quantified per genotype. The mean ± s.e.m. is also shown, $^{***}P<0.001$. SSR size (nm) in control was 695 ± 27 ($n = 59$ boutons) and in muscle Ral^{CA} was 1088 ± 50 ($n = 52$ boutons).

(TEM) on control and Ral^{CA}-expressing muscles. The extent of the SSR can be estimated by measuring the width of the zone of complex membrane infoldings surrounding the presynaptic boutons, from where it contacts the bouton to where the normal cytoplasm of the muscle begins (Figure 2D). Measurements of SSR width by TEM demonstrated Ral-induced SSR growth. The SSR of muscles expressing Ral^{CA} was obviously larger in electron micrographs than that of controls (Figure 2D and E), increasing in width by 56% from 695 ± 27 nm ($n = 58$) to 1088 ± 50 nm ($n = 51$) (Figure 2D and G).

The increase in the SSR was apparent in each Ral^{CA} larva examined and frequently changed the overall appearance of the SSR. Whereas a discrete zone of SSR was normally found around each bouton of a control larva, we encountered several instances in Ral^{CA}-expressing muscles where the SSR formed a continuous zone engulfing multiple boutons (Figure 2F). Also, Ral^{CA} expression gave rise to areas of muscle in which the SSR extended from the synapse deep into the muscle cell, well beyond the immediate vicinity of the presynaptic bouton. Ral^{CA} expression selectively evoked membrane overgrowth of the SSR; total muscle surface area was not changed, invaginations of the membrane were not encountered elsewhere along the muscle surface and other synaptic parameters quantified by TEM were also unchanged (Supplementary Table S1). Localized membrane overgrowth of the SSR is consistent with Ral^{CA} recruitment of the exocyst selectively to the synaptic region.

By using light microscopy, we confirmed the widespread SSR expansion surrounding type I boutons. We expressed CD8-GFP in muscles, an exogenous membrane protein that indiscriminately labels the entire plasma membrane. Because of the abundance of membrane that forms the folds of the SSR, CD8-GFP is brightest where SSR is present. The intensity of this fluorescence surrounding boutons and its thickness thereby reflects the packing density of SSR membrane and SSR thickness. We found that both parameters were increased at the synapse when Ral^{CA} was expressed (Supplementary Figure S2D–I), as expected from the EM. The colocalization of Sec5 and CD8-GFP in muscles expressing Ral^{CA} (Supplementary Figure S2F and G) further supported the possibility that exocyst recruitment to the synapse reflected increased membrane addition for SSR growth. The six-fold increase in Sec5 intensity caused by Ral^{CA} was far greater than the 1.5-fold change in CD8-GFP; thus, the exocyst was actively recruited to the postsynaptic region and not a passive consequence of the presence of more membrane.

sec5 and *ral* mutants have defects in SSR development

To address whether SSR development requires Sec5 and Ral, we examined the structure of the SSR in *sec5* and *ral* mutant larvae. We analysed *sec5* null mutants of which a few can survive for up to 96 h due to maternally contributed protein, but the majority die earlier (Murthy *et al*, 2003). We also analysed two ral mutants: ral^{PG89}, which has been characterized (Balakireva *et al*, 2006) and survives to 60 h and ral^{G0501}, which survives to late pupae but that has not previously been characterized. Both *ral* mutants lacked detectable protein expression by western blot (Supplementary Figure S3A) and were therefore processed for TEM. The SSR of wild-type muscles starts to form around 48 h (early second instar) and continues to grow through the third instar (Supplementary Figure S3B–D). At 60 h, the SSR is reliably present but slightly thinner than that of the third instar and 60 h was therefore chosen as a suitable time point at which to examine the influence of Sec5 and Ral on the rate of its development. *sec5* mutant muscles had only a rudimentary SSR, considerably thinner (149 ± 9 nm in $sec5^{-/-}$) than that of controls (580 ± 33 nm) (Figure 3A, B, and J). In these mutants, only one or two SSR folds were visible around most boutons (Figure 3B); among 34 boutons examined from three *sec5* larvae, only one bouton had a nearly normal thickness of SSR, but it extended only around half the bouton, with the other half lacking SSR (Supplementary Figure S3E). SSR size and complexity were more variable in *ral* mutants ($ral^{PG89} = 240 \pm 20$ nm and $ral^{G0501} = 260 \pm 27$ nm) than in *sec5* mutants, but their SSR was significantly smaller than control larvae (Figure 3C, D, and J; Supplementary Figure S3F and G). Expression of Sec5 or Ral^{WT} back into the mutant larvae fully rescued SSR development (Supplementary Figure S4C–E), confirming that the observed defects are specific to these genes. As in third-instar larvae, Ral^{CA} expression enlarged the SSR of control larvae at 60 h (909 ± 70 nm) (Figure 3E and J). However, when Ral^{CA} was expressed in muscles of *sec5* mutants, no SSR expansion was seen: SSR thickness (158 ± 11 nm) was comparable to that in *sec5* mutants without Ral^{CA} (149 ± 9 nm) (Figure 3F and J). Conversely, expression of UAS-Sec5 in muscles of ral^{PG89} was also not sufficient to rescue SSR formation (Supplementary Figure S4A and B). Thus, development of the SSR is dependent on both Ral and Sec5 and the extent of its growth can be influenced by activated Ral in a Sec5-dependent manner.

We also analysed the phenotypes of third-instar larvae in genotypes that survived to that stage: ral^{G0501} mutants and larvae expressing Sec5 RNAi in the muscle (muscle Sec5-IR) (Supplementary Figure S5). ral^{G0501} third-instar larvae had a very small SSR compared to control and indeed the SSR at this stage was not significantly different from ral^{G0501} mutants (237 ± 27) at 60 h. The decreased SSR therefore is not due to a generalized developmental delay (these larvae survive to pupation) but rather to a selective arrest of SSR growth. Likewise, in the third-instar muscle Sec5-IR, only a rudimentary SSR was observed, which was not different from $sec5^{-/-}$ (Dicer control: 698 ± 44 nm versus muscle Sec5-IR: 167 ± 20 nm) (Figure 3H–J).

In addition, to determine if the synaptic localization of Ral (Figure 1A and B) required Sec5, we immunostained control and $sec5^{-/-}$ muscles expressing Ral^{CA}. Ral^{CA} surrounded the boutons of both genotypes even though there was little or no SSR in the $sec5^{-/-}$ muscles (Figure 3K–L). In control animals, expression of Ral^{CA} induced Sec5 recruitment starting at 48 h and Sec5 levels increased as the SSR expanded at 60 h (Figure 3E). Thus, Ral localization to the synaptic area is upstream of Sec5 activation and does not require Sec5, whereas Sec5 recruitment by Ral^{CA} parallels the growth of the SSR and is required for that growth.

Ca^{2+} influx recruits Sec5 to the synapse

Two pathways that can activate Ral are Ras activation of Ral-GEF (Hofer *et al*, 1994; Kikuchi *et al*, 1994) and direct Ca^{2+}-calmodulin binding to Ral (Hofer *et al*, 1998; Wang and Roufogalis, 1999). To determine if Ras acts in *Drosophila* muscle to recruit Sec5 to the NMJ, we expressed in the muscle a previously characterized transgene for

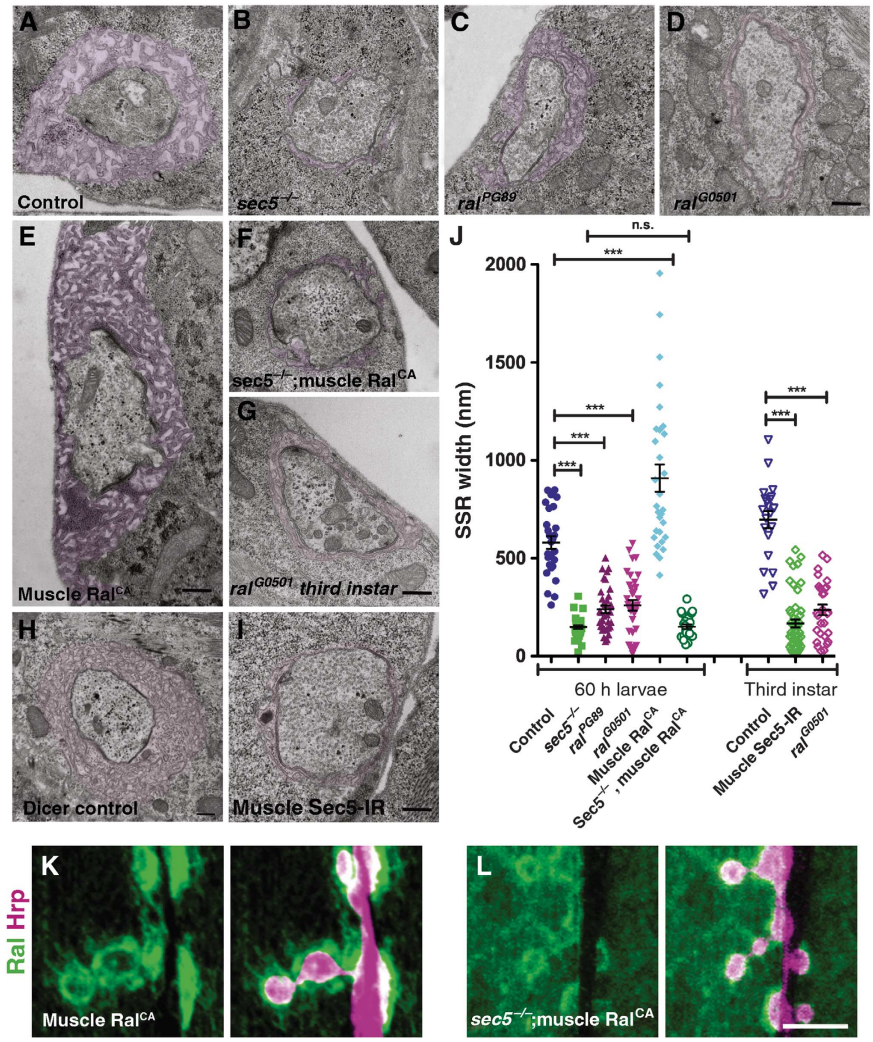

Figure 3 SSR formation depends on *sec5* and *ral*. (**A–I**) Electron microscopy of type Ib boutons in 60 h larvae (**A–F**) from (**A**) control (MHC-Gal4/+), (**B**) $sec5^{E10}/sec5^{ts1}$, (**C**) ral^{PG89}, (**D**) ral^{G0501}, (**E**) muscle Ral^{CA} (MHC-Gal4/UAS-Ral^{CA}), and (**F**) $sec5^{E10}/sec5^{ts1}$; MHCGS-Gal4/UAS-Ral^{CA}, and in third instar from (**G**) ral^{G0501}, (**H**) control (Dicer2/G14-Gal4/+), and (**I**) muscle Sec5-IR (Dicer2/G14-Gal4/UAS-Sec5-IR). The SSR is tinted for ease of visualization. Scale bars are 500 nm. (**J**) Quantification of SSR width (nm) in the genotypes shown in (**A–I**). The mean ± s.e.m. is shown and each point represents the SSR width around an individual type Ib bouton; at least three larvae were quantified per genotype. $***P<0.001$, n.s., not-significant. SSR widths (nm) were control = 580 ± 33 ($n=27$ boutons), $sec5^{-/-}$ = 149 ± 9 ($n=34$ boutons), ral^{PG89} = 240 ± 20 ($n=34$ boutons), ral^{G0501} = 260 ± 27 ($n=34$ boutons), muscle Ral^{CA} = 909 ± 70 ($n=30$ boutons) and $sec5^{-/-}$; MHC-Gal4/UAS-Ral^{CA} = 151 ± 11 ($n=26$ boutons), ral^{G0501}(third) = 237 ± 27 ($n=29$ boutons), control = 698 ± 44 ($n=21$ boutons) and muscle Sec5-IR = 167 ± 20 ($n=51$ boutons). (**K**, **L**) Neuromuscular junctions of 60 h larvae labelled with Ral (green) and the neuronal marker anti-HRP (magenta). Postsynaptic localization of Ral^{CA} was observed in both wild-type (**K**) and $sec5^{-/-}$ (**L**) larvae. Genotypes are MHC-GS-Gal4/Ral^{CA} (**G**) and $sec5^{E10}/sec5^{ts1}$; MHCGS-Gal4/Ral^{CA}. Scale bar is 5 μm.

constitutively active Ras (Ras^{CA}) (Bergmann *et al*, 1998). Ras^{CA} did not cause the synaptic redistribution of Sec5 that was seen with Ral^{CA} expression (Supplementary Figure S6). To examine Ca^{2+}/calmodulin-dependent activation of Ral, we elevated intracellular Ca^{2+} with the Ca^{2+} ionophore calcimycin. Wild-type third-instar larvae were dissected in saline and then treated with calcimycin for 5 min in either 0 or 1 mM Ca^{2+} saline. Calcimycin was removed and the preparations were rested for 15 min in 0 Ca^{2+} before fixation. Ca^{2+} influx via calcimycin treatment significantly recruited Sec5 to the vicinity of the synaptic boutons in a manner that closely resembled the effect of Ral^{CA} expression (Figure 4A–C).

To test whether the Ca^{2+}-induced Sec5 recruitment is mediated by Ral, we compared calcimycin effects on wild-type and ral^{PG89} mutant larvae, size and age matched at ~60 h after egg laying (AEL). In wild-type larvae, Ca^{2+} influx evoked Sec5 recruitment to the NMJ as had been seen in third-instar larvae (Figure 4D, E, and H). In the absence of Ca^{2+} influx, ral^{PG89} larvae were identical to controls; Ral is therefore not necessary for the expression and resting distribution of Sec5. In the *ral* mutant larvae, however, calcimycin treatment failed to recruit Sec5 to the NMJ (Figure 4F–H). Thus, the Ca^{2+}-induced Sec5 recruitment to the NMJ is Ral dependent.

Glutamate or nerve stimulation recruits Sec5 to the NMJ

To determine whether physiologic stimuli that elevate cytosolic Ca^{2+} could activate the Ca^{2+}/Ral pathway, we examined Sec5 distribution upon glutamate application (Figure 5). In 60 h, larval muscles exposed to 30 μM glutamate, Sec5 was

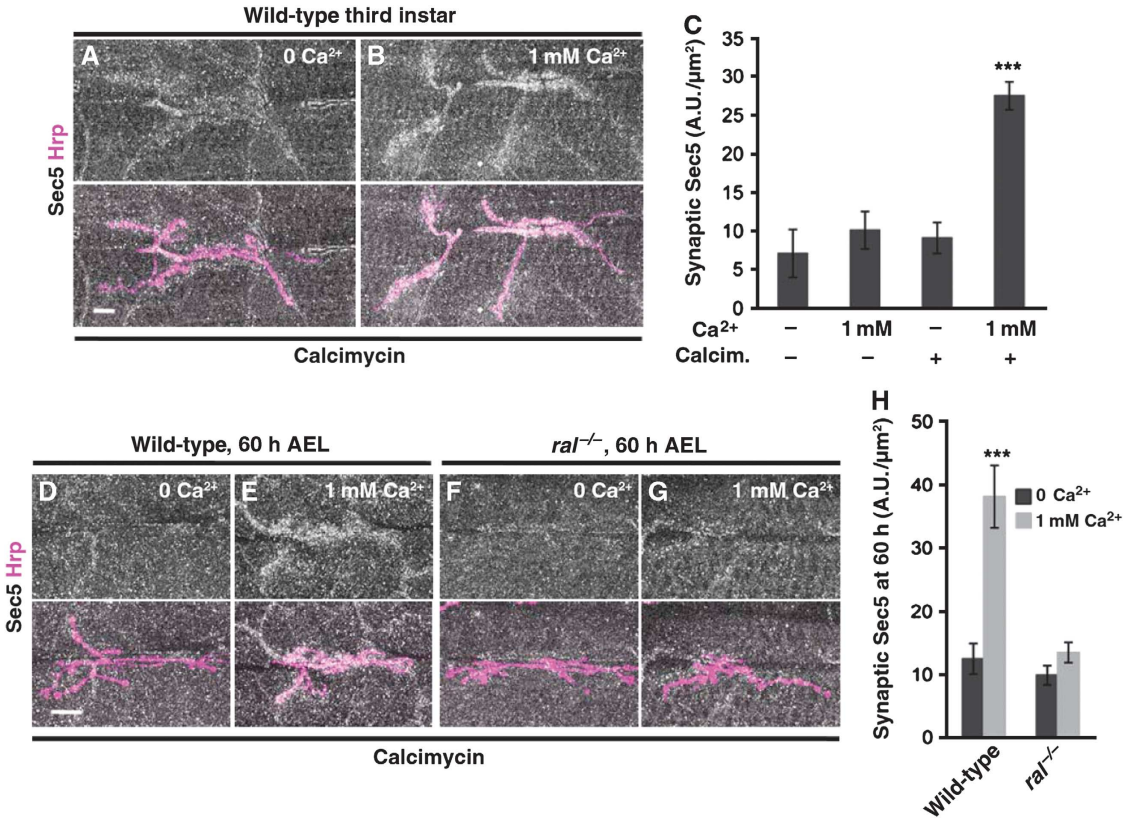

Figure 4 Elevated intracellular Ca^{2+} recruits Sec5 to the NMJ, in a *ral*-dependent manner. (**A**, **B**) Wild-type (w^{1118}) third-instar larvae were treated with calcimycin in either Ca^{2+}-free (**A**) or 1 mM Ca^{2+} (**B**) containing saline and subsequently labelled with anti-Sec5 (grey) and anti-Hrp (magenta). (**C**) Quantification of synaptic enrichment of Sec5 (A.U./μm^2) in the presence and absence of calcimycin and Ca^{2+}. (**D–G**) Sec5 immunoreactivity (grey) was enriched at synapses (anti-HRP labelled; magenta) of second-instar larvae (60 h) upon calcimycin exposure in Ca^{2+}-containing (**E**) or Ca^{2+}-free (**D**) saline. This synaptic recruitment did not occur in $ral^{-/-}$ muscles (**F**, **G**). (**H**) Quantification (mean ± s.e.m.) of the enrichment of synaptic Sec5 (Arbitrary Units/μm^2) from conditions in **D–G**. ***$P<0.001$ in **C**, **H**. Scale bars = 10 μm.

recruited to the NMJ, but only if Ca^{2+} was present in the medium and only in wild-type but not in ral^{PG89}mutant larvae (Figure 5A–D and I). Glutamate application also recruited Sec5 at third-instar NMJs (Figure 5E, F, and J). Thus, Ca^{2+} influx triggered by glutamate-receptor activation can induce Ral-dependent recruitment of Sec5 to synapses.

We used nerve stimulation for a more physiological activation of the glutamate receptors. We expressed the temperature-activated channel dTrpA1 in motor neurons using the driver OK6-Gal4 (Aberle *et al*, 2002; Hamada *et al*, 2008). The channel was activated with application of 37°C saline to the preparation for 5 min, which was subsequently returned to 20°C for 15 min before fixation. Sec5 immunoreactivity was compared to larvae lacking the dTrpA1 transgene but subjected to the same temperature shift. Nerve activation by dTrpA1 potently led to the accumulation of Sec5 at the synapse (Figure 5G, H, and K). As an alternative means of nerve activation, a suction electrode was used to stimulate the nerve for 5 min at 10 Hz in 1 mM Ca^{2+}, which was followed by a 15 min rest period before fixation and immunostaining. Sec5 immunoreactivity was significantly increased at the stimulated synapses relative to the unstimulated side (Supplementary Figure S7). The ability of stimulation by either method to recruit Sec5 to the NMJ is consistent with the ability of glutamate receptors to activate the Ca^{2+}- and Ral-dependent pathway and indicates that this recruitment is likely to occur under normal physiological conditions.

SSR size is modulated by activity

The ability of Ral^{CA} to enlarge the SSR raised the possibility that nerve stimulation over an extended period might accomplish a similar change in this structure. We therefore used the OK6-Gal4 to express UAS-dTrpA1 in motor neurons to increase their firing by increasing the temperature. Conversely, a transgene for a temperature-sensitive, dominant-negative allele of dynamin (UAS-shi^{ts}) was expressed to decrease synaptic transmission. We used two protocols: (1) shifting larvae to 30°C for 48 h and (2) placing them in tubes in a PCR machine and exposing them for 48 h to cycles of 15 min at 30°C followed by 45 min at 20°C. Larval survival was much higher with the latter method but for both methods larvae were 60 h AEL when the protocols were initiated and after the completion of the 48 h, were dissected and processed for TEM. Control larvae were exposed to the same temperature shifts. With either protocol, upregulation or downregulation of activity significantly altered SSR width. When UAS-shi^{ts} was expressed in motor neurons, the SSR was thinner than in control larvae (635 ± 34 versus 789 ± 41 nm for protocol 1, and 586 ± 33 versus 862 ± 57 nm for protocol 2). Conversely, when UAS-dTrpA1 was expressed the SSR was significantly larger than in controls (1247 ± 73 for protocol 1 and 1157 ± 56 nm for protocol 2) (Figure 6; Supplementary Figure S8). We also quantified Syndapin, GluRIIB, and Dlg levels at synapses after submitting the larvae to 48 h of cycling temperatures in the PCR machine. Although these values showed

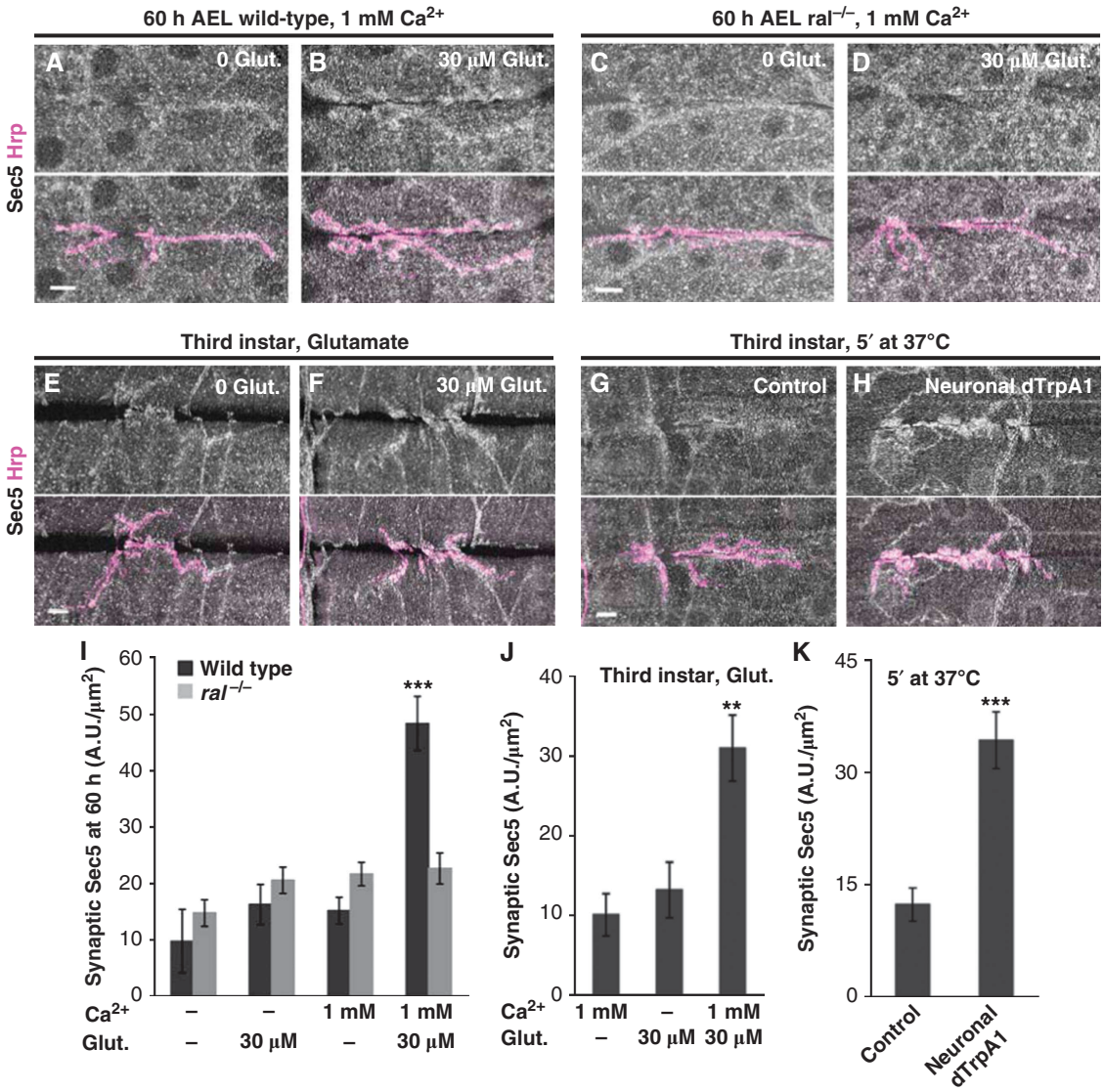

Figure 5 Glutamate-receptor activation and nerve stimulation recruit Sec5 to the NMJ in a Ral-dependent manner. NMJs were labelled with anti-Sec5 (grey) and anti-HRP (magenta). (**A–D**) In the presence of Ca^{2+}, application of glutamate recruited Sec5 to wild-type, but not to $ral^{-/-}$ 60 h NMJs. Wild-type (w^{1118}, **A**, **B**) and $ral^{-/-}$ (ral^{PG89}, **C**, **D**) NMJs were treated for 5 min with 1 mM Ca^{2+} in control saline (**A**, **C**) or 30 μM glutamate (**B**, **D**). (**E**, **F**) Third-instar wild-type larvae (w^{1118}) incubated with 1 mM Ca^{2+} and with (**F**) or without (**E**) 30 μM glutamate. In the presence of Ca^{2+} and glutamate, Sec5 was recruited to the NMJ. (**G**, **H**) Neuronal activity was enhanced by expression of the temperature-activated dTrpA1 (OK6-Gal4/UAS-dTrpA1, **G**) and compared to control larvae subjected to the same temperature regimen but lacking the channel (OK6-Gal4/+, **H**). (**I**) Quantification of the enrichment of synaptic Sec5 (A.U./μm^2) by glutamate receptor activation (as in **A–D**), and in the presence and absence of Ca^{2+}. (**J**) Quantification of synaptic enrichment of Sec5 (A.U./μm^2) in the third instar by Glutamate (as in **E** and **F**) and (**K**) of nerve stimulation by dTrpA1 activation (as in **G** and **H**). Means ± s.e.m. are shown, $^{**}P<0.01$ and $^{***}P<0.001$. Scale bars are 10 μm.

modest changes of the sort that might be expected from activation of the Ral pathway, only the increase in the levels of Syndapin and GluRIIB upon TrpA1 activation reached statistical significance. The effect is weak probably because manipulations with TrpA1 and shi^{ts} are less potent than constant expression of Ral^{CA}. Thus, the SSR is a plastic structure whose size can be regulated by the level of synaptic activity, and the changes in the SSR width correlated well with the ability of activity to recruit the exocyst to the synapse.

$RalA^{CA}$ expression in mammalian neurons increases dendritic spine density

The effect of Ral-mediated exocyst activation on synapse morphology in *Drosophila* raised the possibility that Ral might also influence synaptic growth in mammalian neurons. As a preliminary inquiry into this question, we expressed RalA, the closest homologue of *Drosophila* Ral, in cultured hippocampal neurons. RalA and the exocyst are known to regulate early stages of neuronal development, including neurite formation (Lalli and Hall, 2005). To avoid the early developmental contribution of this pathway, we transfected neurons on the 19th day *in vitro* (DIV), at which time they have already differentiated and formed dendritic spines and synapses (Dotti *et al*, 1988). Three RalA constructs were used: RalA72L-myc ($RalA^{CA}$) which is locked in the GTP-bound state, RalA28N -myc ($RalA^{inact}$) which is locked in the GDP-bound state, and RalA72L/D49E-myc ($Ral^{CA\Delta Exo}$) in which a point mutation that blocks binding to the exocyst

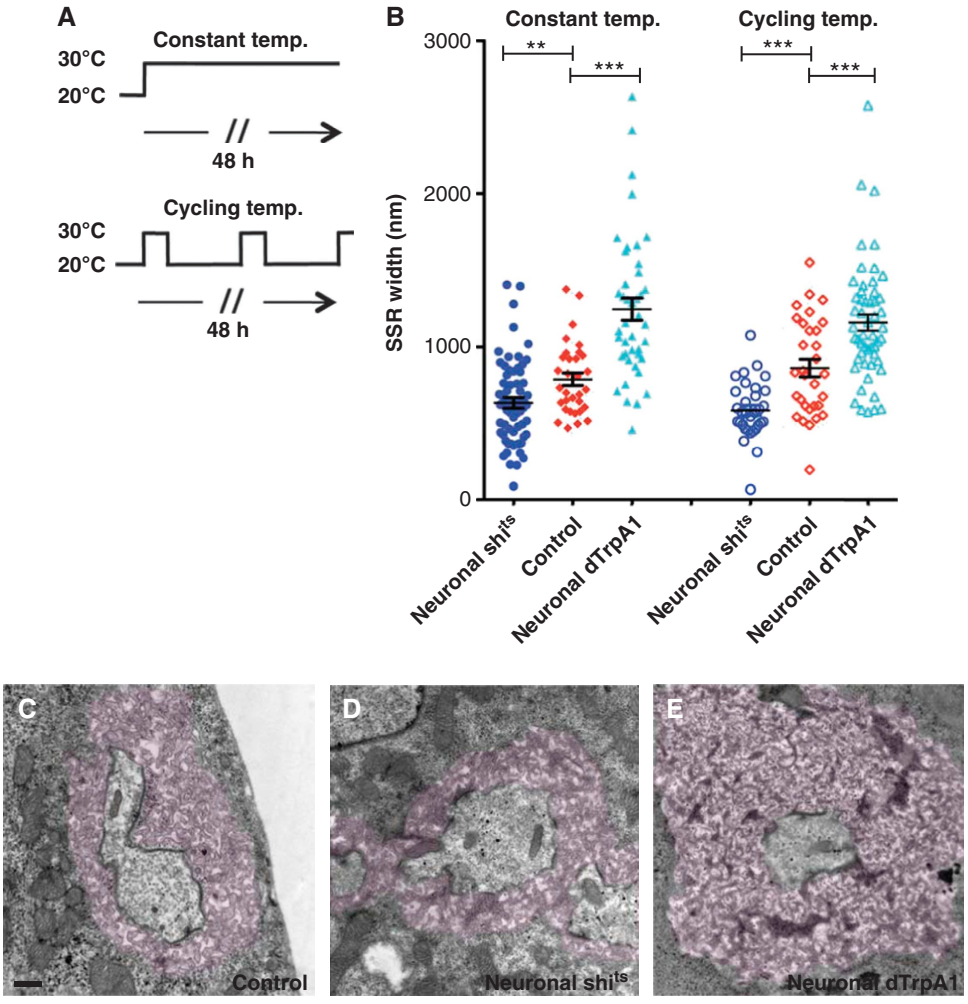

Figure 6 SSR size is modulated by synaptic activity. (**A**) Synaptic activity was manipulated during larval development by expressing in neurons transgenes encoding dTrpA1 to excite neurons or Shi^{ts} to block transmitter release. Two protocols were used, schematized in **A**: (1) A sustained temperature shift of larvae to 30°C for 48 h (filled symbols); (2) Cycling temperatures for 48 h between 15 min at 30°C and 45 min at 20°C (open symbols). (**B**) Quantification of SSR width in nm (mean ± s.e.m.): protocol (1) Shi^{ts} expression 635 ± 34 ($n = 65$), control 789 ± 41 ($n = 32$), dTrpA1 expression 1247 ± 73 ($n = 42$); protocol (2) Shi^{ts} expression 586 ± 33 ($n = 32$), control 862 ± 57 ($n = 31$), neuronal dTrpA1 expression 1157 ± 56 ($n = 53$). $***P < 0.001$, $**P < 0.01$. With either protocol, the SSR was revealed to be an activity-modulated structure: less activity diminished the SSR and greater activity enlarged it. (**C**–**E**) Electron micrographs of the indicated genotypes after the cycling temperature protocol. Scale bar is 500 nm.

components Sec5 and Exo84 has been introduced into the $RalA^{CA}$-myc construct (Lalli and Hall, 2005). These constructs were transfected with DsRed to fill the neurons and reveal their dendrite and spine morphology and PSD95-YFP to mark postsynaptic densities. At 21 DIV, 48 h post transfection, we processed the neurons for immunocytochemistry and quantified the number of spines. All RalA constructs localized to both the cell body and dendrites (Supplementary Figure S9A). Neuronal morphology was not grossly altered by expression of these constructs, although a small but significant decrease in the number of distal branches and an increase in proximal branch density were seen upon $RalA^{CA}$ expression relative to control neurons without a RalA transgene (Supplementary Figure S9B–D). Spine density per μm of dendrite, however, increased 32% when $RalA^{CA}$ was expressed (control = 0.30 ± 0.016 versus $RalA^{CA}$ = 0.39 ± 0.023 spines/μm of dendrite) (Figure 7A and B). In contrast, neither $RalA^{inact}$ nor $RalA^{CA\Delta Exo}$ altered spine density (0.27 ± 0.023 and 0.29 ± 0.022 spine/μm) relative to controls. When only those spines positive for PSD95-YFP were counted, i.e., those that are likely to be part of functional synapses, $RalA^{CA}$ expression caused a 50% increase (Figure 7D) relative to controls or the other RalA transgenes (control = 0.21 ± 0.027, $RalA^{CA}$ = 0.32 ± 0.034, $RalA^{CA\Delta Exo}$ = 0.18 ± 0.029, and $RalA^{inact}$ = 0.23 ± 0.016 spines with PSD95/μm). The increase in PSD95-positive spines after expression of $RalA^{CA}$ relative to $RalA^{inact}$ is also present when endogenous PSD95 rather than the YFP-tagged transgene is used to identify those spines ($RalA^{CA}$ = 0.15 ± 0.015 and $RalA^{inact}$ = 0.07 ± 0.016) (Supplementary Figure S10). Although spine density changed, their average neck length and head diameter did not (Figure 7E and F). In summary, activated RalA expression in hippocampal neurons increased the density of PSD-95-positive spines and this increase was blocked by a mutation that prevents the interaction of RalA with Sec5.

Neuronal depolarization mimics $RalA^{CA}$ expression by promoting Sec5 trafficking into dendritic spines

To further explore whether the Ral/exocyst pathway may also regulate mammalian synaptic structure, we asked whether

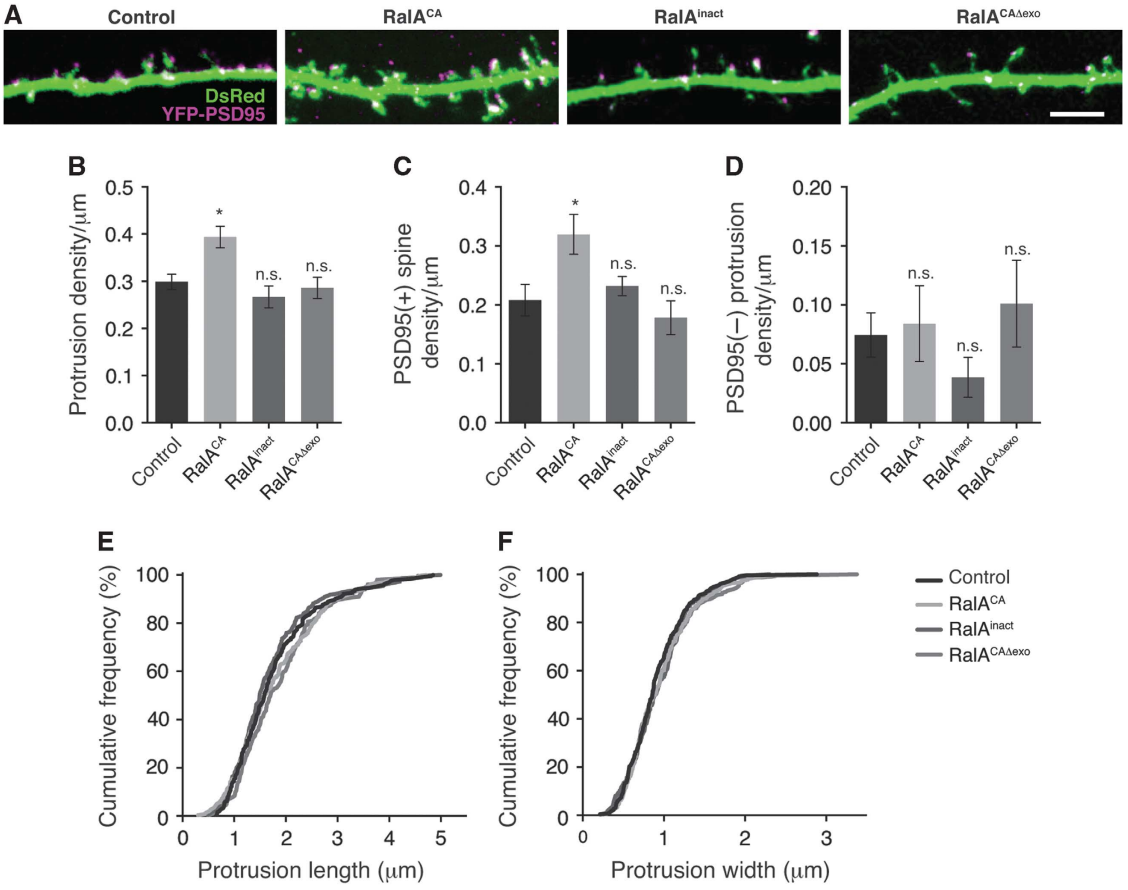

Figure 7 Expression of activated RalA in hippocampal neurons increases spine density. (**A**) Representative dendrites of hippocampal neurons transfected with DsRed, PSD95-YFP, and either constitutively active RalA ($RalA^{CA}$), inactive RalA ($RalA^{inact}$), or constitutively active RalA with a point mutation that blocks binding to the exocyst (abbreviated exo) members Sec5 and Exo84 ($RalA^{CA\Delta exo}$). Only $RalA^{CA}$ increased spine density. DsRed has been pseudo-coloured in green and PSD95-YFP in magenta. (**B**–**D**) Quantification of spine density after transfections as in **A** as determined for total spines (**B**), spines lacking PSD95 (**C**), or spines positive for PSD95 (**D**). (**E**, **F**) Cumulative distribution histograms of spine length and width indicate that RalA alters spine density without changing spine shape. Means ± s.e.m. are shown, $^*P<0.05$. Scale bar is 5 μm.

expression of the RalA constructs would have any impact on exocyst localization. We transfected hippocampal neurons DIV19 with HA-Sec5, GFP, and myc-tagged constructs for $RalA^{CA}$, $RalA^{inact}$, or $Ral^{CA\Delta Exo}$. At DIV21, neurons were processed for immunocytochemistry. The three Ral constructs expressed equivalently well in the neurons analysed (Supplementary Figure S11) and in each case the Sec5 transgene was present throughout the soma and dendrites. However, quantification of HA-Sec5 intensity and distribution revealed that $RalA^{CA}$ expression increased levels of Sec5 in spines, whereas $RalA^{inact}$ and $Ral^{CA\Delta Exo}$ expression did not (Figure 8A–D).

Because synaptic activity caused exocyst redistribution in a Ral-dependent manner in *Drosophila*, we asked whether depolarization of the hippocampal cultures would have a similar effect on HA-Sec5 immunostaining as $RalA^{CA}$ expression. For this, we transfected hippocampal neurons DIV19 with HA-Sec5 and GFP, and 48 h later depolarized the neurons with 60 mM KCl in the medium for 3.5 h. The intensity of HA-Sec5 immunoreactivity was not significantly altered in the neuronal somas, or in dendrites but was significantly increased in spines when compared to untreated neurons (Figure 8E–H). These results suggest that spine anatomical plasticity in the hippocampus may indeed share mechanistic features with the Ral/exocyst pathway we have characterized in *Drosophila*.

Discussion

In this study, we establish that the postsynaptic plasma membrane of the *Drosophila* NMJ is subject to activity-dependent morphological plasticity and identify a pathway that can link synaptic activity to postsynaptic membrane growth: the Ca^{2+}-dependent activation of Ral and consequent recruitment of the exocyst (Figure 9). We show that postsynaptic activation of Ral, but not presynaptic, recruited to the NMJ Sec5, Sec15, Sec3, and Sec8 (Figure 1; Supplementary Figure S1), four components of the exocyst. Because Ral is known to promote the assembly of the exocyst complex, it is likely that functional complexes are recruited. Sec5 recruitment was also stimulated by increasing cytosolic Ca^{2+}, a known activator of Ral. Ca^{2+}-dependent exocyst recruitment could be accomplished with an ionophore, by applying glutamate, or by nerve stimulation either via direct electrical excitation or activation of dTrpA1 channels. Thus, synaptic activity and the resulting influx of Ca^{2+} can recruit

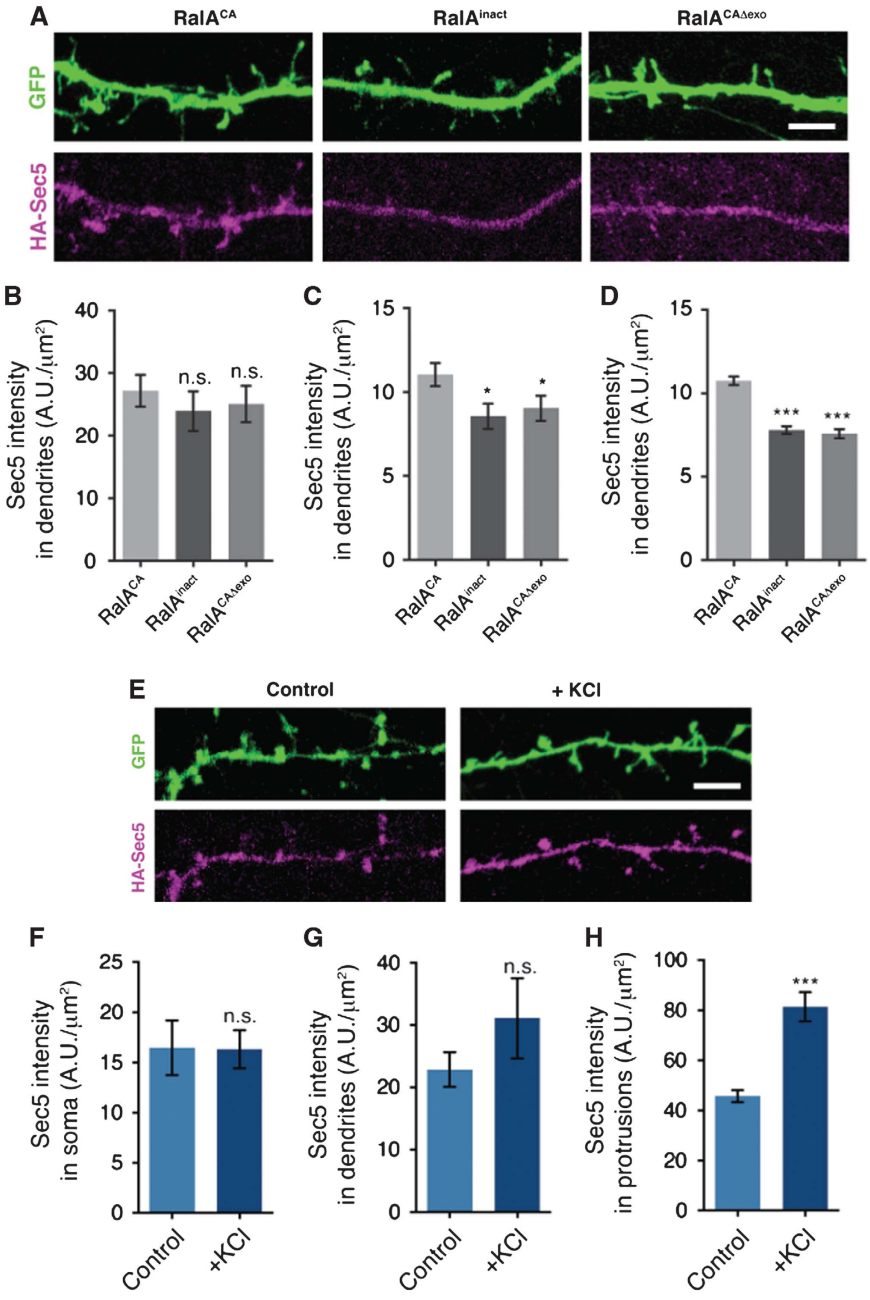

Figure 8 Expression of activated RalA and depolarization cause accumulation of Sec5 in spines. (**A**) Representative dendrites of hippocampal neurons transfected with Sec5 (magenta), GFP (green), and RalA^{CA}, RalA^{inact}, or RalA$^{CA\Delta exo}$. (**B**–**D**) Quantification of Sec5 intensity after transfections as in (**A**), in the cell soma (**B**), dendrites (**C**), and spines (**D**). (**E**) Representative dendrites of hippocampal neurons transfected with Sec5 (magenta), GFP (green) with or without depolarization by KCl. (**F**–**H**) Quantification of Sec5 intensity after depolarization as in **E** the cell soma (**B**), dendrites (**C**), and spines (**D**). All values are in Arbitrary Units and cannot be compared directly between different experiments. The values are shown as mean ± s.e.m. n.s., not significant, $^{*}P<0.05$, $^{***}P<0.0001$. Scale bar represents 5 μm.

Sec5 to the postsynaptic compartment of the muscle fibres (Figures 4 and 5). In *ral* mutant larvae, Ca^{2+} failed to recruit Sec5. The ability of synaptic activity to activate this pathway predicts that activity levels during larval life determine the amount of exocyst-dependent targeting of membrane vesicles to the synaptic region. The significance of chronic activation of the pathway in larval muscle was confirmed by the ability of activated Ral expression to promote enlargement of the membranes of the SSR in an exocyst-dependent fashion, while other aspects of synaptic morphology and composition were unchanged (Figures 2 and 3). Finally, we established that the SSR is indeed a plastic structure whose size is regulated by levels of synaptic activity (Figure 6). Given the ability of synaptic activity to recruit Sec5 to the synapse upon acute stimulation, it seems reasonable to hypothesize that the chronic activation of the pathway during development was responsible for the activity-dependent control of SSR growth (Figure 9).

The SSR is a membrane system conserved in several arthropods (Jahromi and Atwood, 1974; Rheuben, 1985; Feeney *et al*, 1998) that harbours postsynaptic machinery (Ataman *et al*, 2006). Its function is not understood but, given

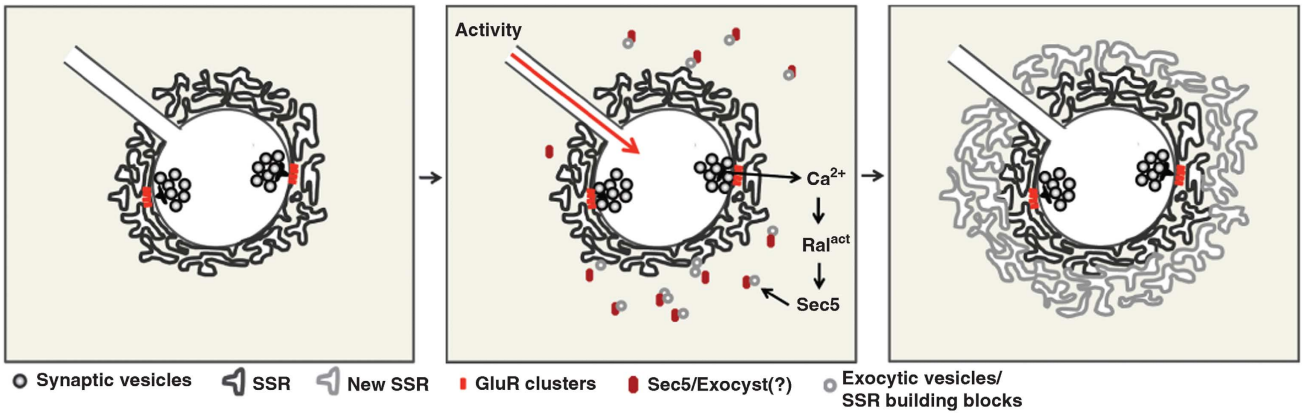

Figure 9 Model of Ral and Exocyst involvement in an activity-driven pathway for postsynaptic membrane addition. Neuronal activity triggers Ca^{2+} entry into the muscle through activation of postsynaptic glutamate receptors and depolarization of the muscle. The increased cytosolic Ca^{2+} activates Ral and the interaction of Ral with Sec5 causes exocyst-associated membrane vesicles to translocate to and fuse at the postsynapse. The addition of this membrane expands the folds of the SSR around each activated bouton.

its architecture, it is possible that it functions in ways akin to those that are ascribed to dendritic spines: sequestering signalling molecules for localized responses to receptor activation and sculpting the electric signals that are propagated into the postsynaptic cell. Our observation that RalA can also act via the exocyst to alter spine number in hippocampal cells represents an additional and provocative similarity. SSR development starts at 48 h during the second instar and continues through the third-instar stage. During this interval, larvae grow considerably and synaptic boutons are added at the NMJ to match the enlargement of the muscle fibres (Ataman *et al*, 2006; Prokop, 2006; Collins and DiAntonio, 2007). Our data indicate a necessary role for the Ral/exocyst pathway in the formation of the SSR that accompanies this growth. Mutations in either *ral* or *sec5* interfered with formation of the SSR and expression of Ral^{CA} in the muscle increased the SSR (Figures 2 and 3). The action of Ral was upstream of the exocyst, because Ral^{CA} could not promote SSR growth in a *sec5* mutant background. Activation of the pathway alone, however, was not sufficient to induce SSR growth: Ral^{CA} expression prior to 48 h AEL, the time point at which the SSR normally starts developing (Supplementary Figure S3B; Guan *et al*, 1996), neither recruited Sec5 to the NMJ nor caused the premature formation of SSR. We hypothesize that components of the SSR are not present in the muscle prior to 48 h and therefore cannot be trafficked to the synapse in response to Ral. It is likely that SSR development entails two components: an unknown developmental signal that initiates transcription and translation of the building blocks and a membrane trafficking mechanism, dependent on Ral and the exocyst, that mediates and modulates the assembly of those components at the synapse. Because the exocyst can direct membrane addition to particular membrane domains (Wu *et al*, 2008; He and Guo, 2009), the Ral/exocyst pathway at the NMJ likely regulates the rate and location of membrane addition, rather than other aspects of SSR development.

The localization of both Ral and the exocyst components to the region surrounding the bouton was a notable feature of this pathway. However, Ral localization to the NMJ was independent of Sec5 and of the nucleotide-bound state of Ral. In addition, expressed Ral concentrated at the synapse prior to SSR growth and Ral is thus well situated to direct vesicle addition to postsynaptic membranes upon activation by Ca^{2+} and when appropriate cargo vesicles have been produced. Sec5, in contrast, was recruited to this region only when Ral was activated. Two lines of evidence demonstrate that this recruitment was a cause and not a consequence of the enlargement of the SSR. First, the growth of the SSR does not occur in *sec5* mutants or when Sec5 is selectively knocked down in the muscle by RNAi. Second, whereas CD8-GFP is always abundant surrounding boutons due to the concentration of membrane in that region, Sec5 moves to the SSR only in response to the activation of Ral.

SSR development is also under the likely control of other signals, including Neuroligin/neurexins (Banovic *et al*, 2010), Pix and Pak (Parnas *et al*, 2001; Albin and Davis, 2004), Dlg and Spectrin (Lahey *et al*, 1994; Budnik *et al*, 1996; Guan *et al*, 1996; Pielage *et al*, 2006), Par-1 (Zhang *et al*, 2007b), and CamKII (Koh *et al*, 1999). In particular, the wingless/wnt pathway modulates SSR development through nuclear signalling and control of the export of nuclear transcripts (Packard *et al*, 2002; Ataman *et al*, 2008; Mosca and Schwarz, 2010; Speese *et al*, 2012). Because the Wnt-ligand Wingless is secreted from the innervating boutons in an activity-dependent manner (Packard *et al*, 2002; Ataman *et al*, 2008) Wnt signalling may act in parallel to the Ca^{2+}/Ral pathway with the former increasing the synthesis of necessary components and the latter stimulating their incorporation into the postsynaptic membrane.

The acquisition of proper synaptic morphology has multiple components and represents an important late stage of synaptic maturation (Bhatt *et al*, 2009; Newpher and Ehlers, 2009). It includes not only the elaboration of postsynaptic specializations such as spines, folds, or the SSR, but also determination of presynaptic bouton number and size, two processes that are also carefully controlled at the fly NMJ (Griffith and Budnik, 2006; Marques and Zhang, 2006). Notably, the Ca^{2+}/Ral/exocyst pathway altered postsynaptic morphology independently of other properties of the NMJ: presynaptic properties including bouton number and size were unaffected when SSR growth was promoted and glutamate receptors were largely unaltered. The increase in the SSR may occur primarily in its deeper folds and this

zone is marked by Syndapin (which was increased surrounding boutons by Ral^{CA} expression) but lacks Dlg (which did not increase). The ability to regulate independently the growth of the postsynaptic membrane is reminiscent of spine dynamics at mammalian synapses, where synaptic contacts can be converted from shaft synapses to spine synapses and where the volume and shape of spines can change in response to activity without necessarily changing synapse number (Alvarez and Sabatini, 2007; Bourne and Harris, 2007; Bhatt *et al*, 2009; Newpher and Ehlers, 2009). We found that spine density was increased by activated RalA and that both activated RalA and neuronal depolarization increase Sec5 in dendritic spines. These findings raise the possibility that the mechanism by which the postsynaptic membrane expands with spine growth in response to glutamate receptor activation (Kwon and Sabatini, 2011) may resemble the Ral/exocyst pathway by which the glutamatergic synapse at the fly NMJ expands its postsynaptic membrane. Indeed spine growth is likely to be a multifaceted event involving regulated changes in cytoskeletal elements, membrane addition, and receptor trafficking under the control of multiple small GTPases (Park *et al*, 2004; Murakoshi *et al*, 2011; Murakoshi and Yasuda, 2012).

Both glutamate receptor activation and Ca^{2+} influx through calcimycin promoted Sec5 recruitment selectively to the vicinity of the synapse (Figures 4 and 5). Calcimycin, however, permeabilizes the entire muscle membrane to Ca^{2+}. That Sec5 was recruited selectively to the NMJ and not uniformly across the muscle surface suggests that a synaptic targeting mechanism must be present independent of the site of Ca^{2+} entry and regardless of whether the Ca^{2+} enters through glutamate receptors or voltage-dependent channels. We propose instead that the targeting is determined by the localization of Ral to the membrane surrounding the boutons, which in turn recruits and activates the exocyst. The subcellular localization of the exocyst in these activated muscles is consistent with the known function of the exocyst in directing post-Golgi vesicles to target membranes for localized membrane addition (Zhang *et al*, 2001; Dupraz *et al*, 2009; He and Guo, 2009; Murthy *et al*, 2010).

Our studies also indicated that some aspects of exocyst function do not require Ral. Although loss of function mutations in *ral* prevented exocyst-dependent SSR growth, other exocyst-catalysed processes persisted. Sec5 is required for neurite outgrowth and bouton addition at the fly NMJ (Murthy *et al*, 2003), but, even though *ral* mutants have reduced synaptic arbors, NMJs were present in $ral^{-/-}$ embryos and the ral^{G0501} allele survives to pupation though no Ral protein is detectable. Moreover, expression of Ral^{CA} in neurons did not alter presynaptic morphology. Similarly, in mammalian neurons, both Ral-dependent and -independent exocyst functions are found. Ral, via the exocyst, promotes neurite branching and participates in establishing neuronal polarity (Lalli and Hall, 2005; Lalli, 2009) but exocyst-mediated AMPA receptor targeting, insertion, and recycling (Sans *et al*, 2003; Gerges *et al*, 2006; Mao *et al*, 2010) are thought to be independent of Ral. Conversely, Ral also has exocyst-independent neuronal functions, including regulation of NMDA receptor endocytosis in response to LTD, via RalBP1 (Han *et al*, 2009). The complex interplay of Ral and the exocyst clearly requires further elucidation.

The identification of a pathway by which synaptic activity can promote growth of postsynaptic membranes at the fly NMJ and the observations that $RalA^{CA}$ expression in hippocampal neurons increases spine density and both Ral^{CA} and depolarization recruit Sec5 to spines, raise the question as to whether the same Ca^{2+}/Ral/exocyst pathway functions at mammalian synapses. Ca^{2+} entry is a consequence of excitatory transmission in the mammalian brain and mammalian neurons contain both Ral and the exocyst (Brymora *et al*, 2001). While RalA activity promotes the outgrowth and branching of neurites in newly dissociated neurons in a Sec5-dependent manner (Lalli and Hall, 2005), at later stages, it may regulate aspects of dendritic spine dynamics. In particular, LTP increases spine volume, a process that requires the addition of membranes whose source remains largely unknown (Cooney *et al*, 2002; Park *et al*, 2006; Bourne and Harris, 2007). As with the growth of the SSR, spine dynamics represent changes in postsynaptic architecture that are not necessarily coupled with the formation of new synaptic contacts. The glutamatergic NMJ of *Drosophila* has provided insight into molecular pathways of synaptic development and function (Collins and DiAntonio, 2007) that are shared with mammalian synapses. Further studies may establish if a mechanism similar to the *Drosophila* pathway reported here might also figure in spine growth or remodelling in mammals.

Materials and methods

Fly stocks and genetics

Flies were raised at 25°C in cages with grape plates and yeast paste for timed collections. The wild-type strain used was w^{1118}, control larvae were obtained by crossing MHC-Gal4 or OK6-Gal4 with either w^{1118}, y, w or FRT40A. Stocks used were UAS-Ral^{WT}, UAS-Ral^{CA}, and UAS-Ral^{inact} (Mirey *et al*, 2003), ral^{PG89} (Balakireva *et al*, 2006), ral^{G0501} (Bloomington Stock Center), UAS-Ras^{CA} (Bergmann *et al*, 1998), MHC-Gal4, MHC-Gal4-Gene-Switch, OK6-Gal4 (Aberle *et al*, 2002), G14-Gal4, UAS-Rab11^{CA}-YFP (Zhang *et al*, 2007a), *y,w;* $sec5^{E10}$ (Murthy *et al*, 2003), *y,w;* $sec5^{ts1}$ (Murthy *et al*, 2010), UAS-Sec5, UAS-Sec5-IR (VDRC- w1118; P(GD13789)v28873), UAS-dTrpA1 (Hamada *et al*, 2008), and 2XUAS-shi^{ts} (Bloomington Stock Center).

Antibody production and immunocytochemistry

A polyclonal antibody against *Drosophila* Ral protein was raised in guinea pig by injection of the entire Ral protein (produced in bacteria as a GST fusion) (Eurogentec, Belgium). For immunocytochemistry, third-instar larval fillets were dissected and fixed in 4% paraformaldehyde (Sigma-Aldrich) for 20 min or in Bouin's fixative solution (Ricca Chemical Company) for 5 min. For Ral immunostaining in 60 h larvae, animals were fed 5 μg/ml RU486 to increase Ral expression. Antibody staining was performed in PBS containing 0.3% Triton X-100 and 10% normal donkey serum. Larvae were incubated overnight at 4°C in primary antibodies, washed for at least 1 h, blocked for 30 min to 1 h and incubated for 2 h at room temperature in secondary antibodies, diluted in blocking solution. Larval fillets were mounted in Vectashield (Vector Labs). The following primary antibodies were used: guinea pig anti-dRal (1:500), mouse anti-Sec5 (1:40) (Murthy *et al*, 2003), guinea pig anti-Sec15 (1:1500) (Mehta *et al*, 2005), guinea pig anti-Syndapin (1:1000) (gift of V Kumar and M Ramaswami), rabbit anti-Dlg (1:10 000) (Koh *et al*, 1999), rabbit anti-GluRIIB (1:2000) (Marrus *et al*, 2004), mouse anti-GluRIIA, (1:50) (Developmental Studies Hybridoma Bank-DSHB), mouse anti-Brp (1:100) (Hofbauer *et al*, 2009), rabbit anti-Synaptotagmin I (1:4000) (Mackler *et al*, 2002), and rabbit anti-Par1 (1:200). Cyanine 5 (Cy5)-, cyanine 3 (Cy3) or FITC-conjugated goat anti-HRP (1:200; Jackson ImmunoResearch) was used to label neuronal membranes; for Sec5 staining, we used minimum crossreactivity DyLight 549-conjugated secondary antibodies (1: 200; Jackson

ImmunoResearch). For all remaining reactions, we used minimum crossreactivity secondaries that were A488-, Cy2-, DyLight 488-, A568- or DyLight 549-conjugated antibodies (1:200, Jackson ImmunoResearch).

Stimulation protocols

Ca^{2+}/calcimycin stimulation. Larvae were dissected in Ca^{2+}-free saline (5 mM Mg^{2+}) (Jan and Jan, 1976). For unstimulated control preparations, this saline included 0.5 mM EGTA. Dissected larvae were then pre-incubated in 50 μM calcimycin/0 mM Ca^{2+} saline for 10 min, after which they were either placed for 5 min in calcimycin/1 mM Ca^{2+} saline or left in the calcimycin/0 mM Ca^{2+} as a control. The larvae were then washed in 0 mM Ca^{2+} saline and left at rest for 15 min. When comparing wild-type and *ral* mutants, 60 h larvae of each genotype were dissected on the same Sylgard-coated slide and processed together to ensure equivalent treatments.

Glutamate stimulation. Larvae were dissected in Ca^{2+}-free saline (Jan and Jan, 1976) and then exposed for 5 min to 1 mM Ca^{2+} saline with or without 30 μM Glutamate (Glutamic Acid, Sigma Aldrich), followed by 15 min rest in 1 mM Ca^{2+} saline. Larvae were then fixed and processed for immunocytochemistry.

Stimulation of motorneurons using UAS-dTrpA1. OK6-Gal4 larvae were crossed to w^{1118} or to UAS-dTrpA1 flies and kept at 22°C. Third-instar larvae from the two sets of crosses were dissected at room temperature in Ca^{2+}-free saline (Jan and Jan, 1976) and then incubated for 5 min in 1 mM Ca^{2+} saline prewarmed to 37°C. The warm solution was then replaced by a 20°C solution for 15 min prior to fixation.

Manipulations of activity of larval motorneurons. For the temperature cycling paradigm, 60 h larvae of control (OK6-Gal4/+), OK6-Gal4/UAS-dTrpA1, or OK6-Gal4/UAS-shi^{ts} were placed in perforated PCR tubes with yeast paste, and subjected to a regimen of 15 min at 30°C followed by 45 min at 20°C for a total of 48 h in a PCR machine (Eppendorf Mastercycler Pro). Larvae (now at the third instar) were dissected and processed for TEM. For the constant temperature shift, the same genotypes were transferred to 30°C for a 48 h period, after which the third-instar larvae were dissected and processed. Few OK6/TrpA1 larvae survived the sustained 30°C for 48 h, but in the cycling protocol viability was good and equivalent for each genotype.

Electron microscopy

Larvae aged 48 ± 1 h, 60 ± 1 h, or 66 ± 1 h, or wandering third instars were dissected in cold 0.1 M cacodylate buffer. Third-instar larvae were fixed at 4°C overnight in 2.5% paraformaldehyde, 5.0% glutaraldehyde, 0.06% picric acid in 0.1 M cacodylate buffer. Second-instar larvae were processed similarly but fixed for 1 h at room temperature. For the analysis of second instars, each genotype was collected at 60 h but $sec5^{-/-}$ larvae were small, resembling 48 h controls. Larvae were processed for TEM as previously reported (Mosca and Schwarz, 2010). Ultrathin sections were taken parallel to the surface of the muscles and were mounted on single slot grids, stained with lead and uranyl acetate, and imaged on a Tecnai G^2 Spirit BioTWIN (FEI Company) electron microscope. A minimum of three larvae were quantified per genotype.

Image quantification

Larvae were imaged on a Zeiss LSM 510 Meta laser scanning confocal microscope (Carl Zeiss, Oberkochen, Germany) with a 63 × 1.4 NA objective. Optical sections were 1 μm except for Figures 1A, B, 3K, and L and Supplementary Figure S2F and G, which were 0.5 μm. Images were processed in separate channels using the LSM software or Adobe Photoshop CS4 (Adobe Systems, San Jose, CA). Each experiment was repeated at least three independent times and quantified data are always from at least four different larvae, segments A2 and A3, and a minimum of eight NMJs. For each set of quantification, data were acquired with identical settings and analysed as 8-byte images, maximum projection, with the same settings, using Fiji/ImageJ (NIH, Bethesda, Maryland).

Quantification of Sec5 and other synaptic markers. To define the perisynaptic region, anti-HRP staining was thresholded so as to outline synaptic boutons. For quantification of Sec5, threshold settings and parameters were kept constant for all data points. After thresholding, the HRP-positive area was expanded by 2 μm (5 iterations on ImageJ) to form a synaptic region of interest that contained the postsynaptic region and within which the intensity of the Sec5 immunostaining could be quantified. The integrated fluorescence intensity was normalized to the area of the region of interest for total Sec5 at NMJ/μm^2. To determine the degree of enrichment at the synapse, intensity/area of Sec5 immunostaining was also measured in a non-synaptic region of the muscle in an area of at least 10 × 10 μm. Synaptic Sec5 enrichment was defined as the difference between the normalized intensities of the synaptic and non-synaptic regions. To quantify other postsynaptic markers (Figure 2), we also measured intensity of immunofluorescence within an expanded region around the boutons, but for pre-synaptic markers, the anti-HRP-positive area was not expanded. All values in Figure 2A are expressed as a percentage of the intensity in control larvae.

TEM analysis of SSR thickness. To quantify SSR thickness, micrographs were analysed using Fiji/ImageJ (NIH, Bethesda, Maryland). Boutons were identified by the presence of synaptic vesicles and active zones and eight straight lines, at 45° angles from one another, were drawn from the centre of the bouton. The width of the SSR along each of these radii was measured and a value for each bouton was derived from the average of the eight radii.

Statistic analysis. Statistical analysis was conducted using Excel (Microsoft Corporation, 2007) or GraphPad Prism 6 software (Graphpad Software, La Jolla, CA) and significance values calculated using a two-tailed unpaired t-test or, when more than two samples were compared, a one-way analysis of variance (ANOVA) test followed by *post hoc* Bonferroni test. If our measurements of SSR thickness did not clearly fit a normal distribution (as visualized with a qqplot), and were instead positively skewed, then we applied a log transformation to those data sets to convert them to a symmetrical distribution. The transformed data could then be processed using parametric *t*-tests or ANOVA. All histograms and measurements are shown as mean ± s.e.m.; sample size (n) is described either in the figure legend or in Results section.

Hippocampal culture, transfection, and immunostaining

Primary hippocampal cultures were prepared from embryonic day 18 (E18) Long-Evans rat brains as described previously (Xia *et al*, 1996). Cells were plated on coverslips (Bellco Glass, Inc., Vineland, NJ) coated with poly-ornithine and laminin at a density of 1×10^5/cm^2. Transfections were done using Lipofectamine™ 2000 (Life Technologies, Carlsbad, CA) at DIV19. Two days post transfection (DIV21) neurons were fixed and immunostained as described previously (Tolias *et al*, 2007). Images were acquired with a Zeiss LSM510 confocal microscope (Zeiss, Thornwood, NY) using a 63 × 1.4 NA objective for spine analysis and 40 × 1.3 NA objective for Sholl analysis. For details of constructs, antibodies, image acquisition parameters, and analysis, see Supplementary data.

Supplementary data

Supplementary data are available at *The EMBO Journal* Online (http://www.embojournal.org).

Acknowledgements

This work was supported by National Institutes of Health (NIH) Grants RO1 NS041062 and MH075058 (TLS), the IDDRC Imaging Core (P30HD18655), Harvard Neurodiscovery Imaging Center, and the HMS Conventional Electron Microscopy Facility. We thank X Chen, A Saltiel, G Lalli, H Bellen, V Kumar, M Ramaswami, H Stellar, Vivian Budnik, A DiAntonio, Y Jan, L Zipursky, P Garrity and the Developmental Studies Hybridoma Bank and Bloomington *Drosophila* Stock Center for DNA constructs, antibodies, and fly stocks; Ann Goldstein for fruitful discussions and comments; and David Van Vactor, Elizabeth McNeill, and members of the Schwarz laboratory for critical comments on the manuscript.

Author contributions: ROT and TLS designed all experiments and wrote the manuscript. GP, ROT, AN, and TLS designed and analysed the experiments for Figures 7 and 8; Supplementary Figures S9–S11, GP and AN conducted these experiments. MEHK conducted and analysed the electrophysiology experiments in Supplementary Figure S2A. MB and JC designed and produced the anti-dRal antibody. IGM conducted and analysed the data for Supplementary Figure S7. ROT conducted and analysed all other experiments.

Conflict of interest

The authors declare that they have no conflict of interest.

References

Aberle H, Haghighi AP, Fetter RD, McCabe BD, Magalhaes TR, Goodman CS (2002) wishful thinking encodes a BMP type II receptor that regulates synaptic growth in Drosophila. *Neuron* **33:** 545–558

Albin SD, Davis GW (2004) Coordinating structural and functional synapse development: postsynaptic p21-activated kinase independently specifies glutamate receptor abundance and postsynaptic morphology. *J Neurosci* **24:** 6871–6879

Alvarez VA, Sabatini BL (2007) Anatomical and physiological plasticity of dendritic spines. *Annu Rev Neurosci* **30:** 79–97

Ataman B, Ashley J, Gorczyca M, Ramachandran P, Fouquet W, Sigrist SJ, Budnik V (2008) Rapid activity-dependent modifications in synaptic structure and function require bidirectional Wnt signaling. *Neuron* **57:** 705–718

Ataman B, Budnik V, Thomas U (2006) Scaffolding proteins at the Drosophila neuromuscular junction. *Int Rev Neurobiol* **75:** 181–216

Balakireva M, Rosse C, Langevin J, Chien YC, Gho M, Gonzy-Treboul G, Voegeling-Lemaire S, Aresta S, Lepesant JA, Bellaiche Y, White M, Camonis J (2006) The Ral/exocyst effector complex counters c-Jun N-terminal kinase-dependent apoptosis in Drosophila melanogaster. *Mol Cell Biol* **26:** 8953–8963

Banovic D, Khorramshahi O, Owald D, Wichmann C, Riedt T, Fouquet W, Tian R, Sigrist SJ, Aberle H (2010) Drosophila neuroligin 1 promotes growth and postsynaptic differentiation at glutamatergic neuromuscular junctions. *Neuron* **66:** 724–738

Bergmann A, Agapite J, McCall K, Steller H (1998) The Drosophila gene hid is a direct molecular target of Ras-dependent survival signaling. *Cell* **95:** 331–341

Beronja S, Laprise P, Papoulas O, Pellikka M, Sisson J, Tepass U (2005) Essential function of Drosophila Sec6 in apical exocytosis of epithelial photoreceptor cells. *J Cell Biol* **169:** 635–646

Bhatt DH, Zhang S, Gan WB (2009) Dendritic spine dynamics. *Annu Rev Physiol* **71:** 261–282

Bourne J, Harris KM (2007) Do thin spines learn to be mushroom spines that remember? *Curr Opin Neurobiol* **17:** 381–386

Boyd C, Hughes T, Pypaert M, Novick P (2004) Vesicles carry most exocyst subunits to exocytic sites marked by the remaining two subunits, Sec3p and Exo70p. *J Cell Biol* **167:** 889–901

Brymora A, Valova VA, Larsen MR, Roufogalis BD, Robinson PJ (2001) The brain exocyst complex interacts with RalA in a GTP-dependent manner: identification of a novel mammalian Sec3 gene and a second Sec15 gene. *J Biol Chem* **276:** 29792–29797

Budnik V, Koh YH, Guan B, Hartmann B, Hough C, Woods D, Gorczyca M (1996) Regulation of synapse structure and function by the Drosophila tumor suppressor gene dlg. *Neuron* **17:** 627–640

Chen XW, Leto D, Xiao J, Goss J, Wang Q, Shavit JA, Xiong T, Yu G, Ginsburg D, Toomre D, Xu Z, Saltiel AR (2011) Exocyst function is regulated by effector phosphorylation. *Nat Cell Biol* **13:** 580–588

Collins CA, DiAntonio A (2007) Synaptic development: insights from Drosophila. *Curr Opin Neurobiol* **17:** 35–42

Cooney JR, Hurlburt JL, Selig DK, Harris KM, Fiala JC (2002) Endosomal compartments serve multiple hippocampal dendritic spines from a widespread rather than a local store of recycling membrane. *J Neurosci* **22:** 2215–2224

Davis GW, Bezprozvanny I (2001) Maintaining the stability of neural function: a homeostatic hypothesis. *Annu Rev Physiol* **63:** 847–869

Dickman D, Horne JA, Meinertzhagen IA, Schwarz TL (2005) A slowed classical pathway rather than kiss-and-run mediates endocytosis at synapses lacking synaptojanin and endophilin. *Cell* **123:** 521–533

Dotti CG, Sullivan CA, Banker GA (1988) The establishment of polarity by hippocampal neurons in culture. *J Neurosci* **8:** 1454–1468

Dupraz S, Grassi D, Bernis ME, Sosa L, Bisbal M, Gastaldi L, Jausoro I, Caceres A, Pfenninger KH, Quiroga S (2009) The TC10-Exo70 complex is essential for membrane expansion and axonal specification in developing neurons. *J Neurosci* **29:** 13292–13301

Feeney CJ, Karunanithi S, Pearce J, Govind CK, Atwood HL (1998) Motor nerve terminals on abdominal muscles in larval flesh flies, Sarcophaga bullata: comparisons with Drosophila. *J Comp Neurol* **402:** 197–209

Fukai S, Matern HT, Jagath JR, Scheller RH, Brunger AT (2003) Structural basis of the interaction between RalA and Sec5, a subunit of the sec6/8 complex. *EMBO J* **22:** 3267–3278

Gerges NZ, Backos DS, Rupasinghe CN, Spaller MR, Esteban JA (2006) Dual role of the exocyst in AMPA receptor targeting and insertion into the postsynaptic membrane. *EMBO J* **25:** 1623–1634

Griffith LC, Budnik V (2006) Plasticity and second messengers during synapse development. *Int Rev Neurobiol* **75:** 237–265

Guan B, Hartmann B, Kho YH, Gorczyca M, Budnik V (1996) The Drosophila tumor suppressor gene, dlg, is involved in structural plasticity at a glutamatergic synapse. *Curr Biol* **6:** 695–706

Hamada FN, Rosenzweig M, Kang K, Pulver SR, Ghezzi A, Jegla TJ, Garrity PA (2008) An internal thermal sensor controlling temperature preference in Drosophila. *Nature* **454:** 217–220

Han K, Kim MH, Seeburg D, Seo J, Verpelli C, Han S, Chung HS, Ko J, Lee HW, Kim K, Heo WD, Meyer T, Kim H, Sala C, Choi SY, Sheng M, Kim E (2009) Regulated RalBP1 binding to RalA and PSD-95 controls AMPA receptor endocytosis and LTD. *PLoS Biol* **7:** e1000187

Hanus C, Ehlers MD (2008) Secretory outposts for the local processing of membrane cargo in neuronal dendrites. *Traffic* **9:** 1437–1445

Harvey CD, Yasuda R, Zhong H, Svoboda K (2008) The spread of Ras activity triggered by activation of a single dendritic spine. *Science* **321:** 136–140

Hase K, Kimura S, Takatsu H, Ohmae M, Kawano S, Kitamura H, Ito M, Watarai H, Hazelett CC, Yeaman C, Ohno H (2009) M-Sec promotes membrane nanotube formation by interacting with Ral and the exocyst complex. *Nat Cell Biol* **11:** 1427–1432

He B, Guo W (2009) The exocyst complex in polarized exocytosis. *Curr Opin Cell Biol* **21:** 537–542

Heckscher ES, Fetter RD, Marek KW, Albin SD, Davis GW (2007) NF-kappaB, IkappaB, and IRAK control glutamate receptor density at the Drosophila NMJ. *Neuron* **55:** 859–873

Hofbauer A, Ebel T, Waltenspiel B, Oswald P, Chen YC, Halder P, Biskup S, Lewandrowski U, Winkler C, Sickmann A, Buchner S, Buchner E (2009) The Wuerzburg hybridoma library against Drosophila brain. *J Neurogenet* **23:** 78–91

Hofer F, Berdeaux R, Martin GS (1998) Ras-independent activation of Ral by a Ca(2+)-dependent pathway. *Curr Biol* **8:** 839–842

Hofer F, Fields S, Schneider C, Martin GS (1994) Activated Ras interacts with the Ral guanine nucleotide dissociation stimulator. *Proc Natl Acad Sci USA* **91:** 11089–11093

Holtmaat A, Svoboda K (2009) Experience-dependent structural synaptic plasticity in the mammalian brain. *Nat Rev Neurosci* **10:** 647–658

Huber LA, Ullrich O, Takai Y, Lutcke A, Dupree P, Olkkonen V, Virta H, de Hoop MJ, Alexandrov K, Peter M, Zerial M, Simons K (1994) Mapping of Ras-related GTP-binding proteins by GTP

overlay following two-dimensional gel electrophoresis. *Proc Natl Acad Sci USA* **91:** 7874–7878

Jahromi SS, Atwood HL (1974) Three-dimensional ultrastructure of the crayfish neuromuscular apparatus. *J Cell Biol* **63:** 599–613

Jan LY, Jan YN (1976) Properties of the larval neuromuscular junction in Drosophila melanogaster. *J Physiol* **262:** 189–214

Jin R, Junutula JR, Matern HT, Ervin KE, Scheller RH, Brunger AT (2005) Exo84 and Sec5 are competitive regulatory Sec6/8 effectors to the RalA GTPase. *EMBO J* **24:** 2064–2074

Jin Y, Sultana A, Gandhi P, Franklin E, Hamamoto S, Khan AR, Munson M, Schekman R, Weisman LS (2011) Myosin V transports secretory vesicles via a Rab GTPase cascade and interaction with the exocyst complex. *Dev Cell* **21:** 1156–1170

Kasai H, Fukuda M, Watanabe S, Hayashi-Takagi A, Noguchi J (2010) Structural dynamics of dendritic spines in memory and cognition. *Trends Neurosci* **33:** 121–129

Kelly EE, Horgan CP, McCaffrey MW, Young P (2011) The role of endosomal-recycling in long-term potentiation. *Cell Mol Life Sci* **68:** 185–194

Kennedy MJ, Davison IG, Robinson CG, Ehlers MD (2010) Syntaxin-4 defines a domain for activity-dependent exocytosis in dendritic spines. *Cell* **141:** 524–535

Kennedy MJ, Ehlers MD (2006) Organelles and trafficking machinery for postsynaptic plasticity. *Annu Rev Neurosci* **29:** 325–362

Kikuchi A, Demo SD, Ye ZH, Chen YW, Williams LT (1994) ralGDS family members interact with the effector loop of ras p21. *Mol Cell Biol* **14:** 7483–7491

Koh YH, Popova E, Thomas U, Griffith LC, Budnik V (1999) Regulation of DLG localization at synapses by CaMKII-dependent phosphorylation. *Cell* **98:** 353–363

Kumar V, Fricke R, Bhar D, Reddy-Alla S, Krishnan KS, Bogdan S, Ramaswami M (2009) Syndapin promotes formation of a postsynaptic membrane system in Drosophila. *Mol Biol Cell* **20:** 2254–2264

Kwon HB, Sabatini BL (2011) Glutamate induces de novo growth of functional spines in developing cortex. *Nature* **474:** 100–104

Lahey T, Gorczyca M, Jia XX, Budnik V (1994) The Drosophila tumor suppressor gene dlg is required for normal synaptic bouton structure. *Neuron* **13:** 823–835

Lalli G (2009) RalA and the exocyst complex influence neuronal polarity through PAR-3 and aPKC. *J Cell Sci* **122:** 1499–1506

Lalli G, Hall A (2005) Ral GTPases regulate neurite branching through GAP-43 and the exocyst complex. *J Cell Biol* **171:** 857–869

Liebl FL, Chen K, Karr J, Sheng Q, Featherstone DE (2005) Increased synaptic microtubules and altered synapse development in Drosophila sec8 mutants. *BMC Biol* **3:** 27

Lipschutz JH, Mostov KE (2002) Exocytosis: the many masters of the exocyst. *Curr Biol* **12:** R212–R214

Mackler JM, Drummond JA, Loewen CA, Robinson IM, Reist NE (2002) The C(2)B Ca(2+)-binding motif of synaptotagmin is required for synaptic transmission *in vivo*. *Nature* **418:** 340–344

Mao L, Takamiya K, Thomas G, Lin DT, Huganir RL (2010) GRIP1 and 2 regulate activity-dependent AMPA receptor recycling via exocyst complex interactions. *Proc Natl Acad Sci USA* **107:** 19038–19043

Marques G, Zhang B (2006) Retrograde signaling that regulates synaptic development and function at the Drosophila neuromuscular junction. *Int Rev Neurobiol* **75:** 267–285

Marrus SB, Portman SL, Allen MJ, Moffat KG, DiAntonio A (2004) Differential localization of glutamate receptor subunits at the Drosophila neuromuscular junction. *J Neurosci* **24:** 1406–1415

Martin AR (1955) A further study of the statistical composition on the end-plate potential. *J Physiol (Lond)* **130:** 114–122

Mehta SQ, Hiesinger PR, Beronja S, Zhai RG, Schulze KL, Verstreken P, Cao Y, Zhou Y, Tepass U, Crair MC, Bellen HJ (2005) Mutations in Drosophila sec15 reveal a function in neuronal targeting for a subset of exocyst components. *Neuron* **46:** 219–232

Mirey G, Balakireva M, L'Hoste S, Rosse C, Voegeling S, Camonis J (2003) A Ral guanine exchange factor-Ral pathway is conserved in Drosophila melanogaster and sheds new light on the connectivity of the Ral, Ras, and Rap pathways. *Mol Cell Biol* **23:** 1112–1124

Mosca TJ, Schwarz TL (2010) The nuclear import of Frizzled2-C by Importins-beta11 and alpha2 promotes postsynaptic development. *Nat Neurosci* **13:** 935–943

Moskalenko S, Henry DO, Rosse C, Mirey G, Camonis JH, White MA (2002) The exocyst is a Ral effector complex. *Nat Cell Biol* **4:** 66–72

Moskalenko S, Tong C, Rosse C, Mirey G, Formstecher E, Daviet L, Camonis J, White MA (2003) Ral GTPases regulate exocyst assembly through dual subunit interactions. *J Biol Chem* **278:** 51743–51748

Mott HR, Nietlispach D, Hopkins LJ, Mirey G, Camonis JH, Owen D (2003) Structure of the GTPase-binding domain of Sec5 and elucidation of its Ral binding site. *J Biol Chem* **278:** 17053–17059

Munson M, Novick P (2006) The exocyst defrocked, a framework of rods revealed. *Nat Struct Mol Biol* **13:** 577–581

Murakoshi H, Wang H, Yasuda R (2011) Local, persistent activation of Rho GTPases during plasticity of single dendritic spines. *Nature* **472:** 100–104

Murakoshi H, Yasuda R (2012) Postsynaptic signaling during plasticity of dendritic spines. *Trends Neurosci* **35:** 135–143

Murthy M, Garza D, Scheller RH, Schwarz TL (2003) Mutations in the exocyst component Sec5 disrupt neuronal membrane traffic, but neurotransmitter release persists. *Neuron* **37:** 433–447

Murthy M, Teodoro RO, Miller TP, Schwarz TL (2010) Sec5, a member of the exocyst complex, mediates Drosophila embryo cellularization. *Development* **137:** 2773–2783

Newpher TM, Ehlers MD (2009) Spine microdomains for postsynaptic signaling and plasticity. *Trends Cell Biol* **19:** 218–227

Ngsee JK, Elferink LA, Scheller RH (1991) A family of ras-like GTP-binding proteins expressed in electromotor neurons. *J Biol Chem* **266:** 2675–2680

Packard M, Koo ES, Gorczyca M, Sharpe J, Cumberledge S, Budnik V (2002) The Drosophila Wnt, wingless, provides an essential signal for pre- and postsynaptic differentiation. *Cell* **111:** 319–330

Park M, Penick EC, Edwards JG, Kauer JA, Ehlers MD (2004) Recycling endosomes supply AMPA receptors for LTP. *Science* **305:** 1972–1975

Park M, Salgado JM, Ostroff L, Helton TD, Robinson CG, Harris KM, Ehlers MD (2006) Plasticity-induced growth of dendritic spines by exocytic trafficking from recycling endosomes. *Neuron* **52:** 817–830

Parnas D, Haghighi AP, Fetter RD, Kim SW, Goodman CS (2001) Regulation of postsynaptic structure and protein localization by the Rho-type guanine nucleotide exchange factor dPix. *Neuron* **32:** 415–424

Peng J, Kim MJ, Cheng D, Duong DM, Gygi SP, Sheng M (2004) Semiquantitative proteomic analysis of rat forebrain postsynaptic density fractions by mass spectrometry. *J Biol Chem* **279:** 21003–21011

Pielage J, Fetter RD, Davis GW (2006) A postsynaptic spectrin scaffold defines active zone size, spacing, and efficacy at the Drosophila neuromuscular junction. *J Cell Biol* **175:** 491–503

Prokop A (2006) Organization of the efferent system and structure of neuromuscular junctions in Drosophila. *Int Rev Neurobiol* **75:** 71–90

Rao Y, Ma Q, Vahedi-Faridi A, Sundborger A, Pechstein A, Puchkov D, Luo L, Shupliakov O, Saenger W, Haucke V (2010) Molecular basis for SH3 domain regulation of F-BAR-mediated membrane deformation. *Proc Natl Acad Sci USA* **107:** 8213–8218

Rheuben MB (1985) Quantitative comparison of the structural features of slow and fast neuromuscular junctions in Manduca. *J Neurosci* **5:** 1704–1716

Rheuben MB, Yoshihara M, Kidokoro Y (1999) Ultrastructural correlates of neuromuscular junction development. *Int Rev Neurobiol* **43:** 69–92

Sans N, Prybylowski K, Petralia RS, Chang K, Wang YX, Racca C, Vicini S, Wenthold RJ (2003) NMDA receptor trafficking through an interaction between PDZ proteins and the exocyst complex. *Nat Cell Biol* **5:** 520–530

Speese SD, Ashley J, Jokhi V, Nunnari J, Barria R, Li Y, Ataman B, Koon A, Chang YT, Li Q, Moore MJ, Budnik V (2012) Nuclear envelope budding enables large ribonucleoprotein particle export during synaptic Wnt signaling. *Cell* **149:** 832–846

Steiner P, Sarria JC, Huni B, Marsault R, Catsicas S, Hirling H (2002) Overexpression of neuronal Sec1 enhances axonal branching in hippocampal neurons. *Neuroscience* **113:** 893–905

Stewart BA, Atwood HL, Renger JJ, Wang J, Wu CF (1994) Improved stability of Drosophila larval neuromuscular preparations in haemolymph-like physiological solutions. *J Comp Physiol A* **175:** 179–191

Sugihara K, Asano S, Tanaka K, Iwamatsu A, Okawa K, Ohta Y (2002) The exocyst complex binds the small GTPase RalA to mediate filopodia formation. *Nat Cell Biol* **4:** 73–78

Tada T, Sheng M (2006) Molecular mechanisms of dendritic spine morphogenesis. *Curr Opin Neurobiol* **16:** 95–101

Tolias KF, Bikoff JB, Kane CG, Tolias CS, Hu L, Greenberg ME (2007) The Rac1 guanine nucleotide exchange factor Tiam1 mediates EphB receptor-dependent dendritic spine development. *Proc Natl Acad Sci USA* **104:** 7265–7270

Vega IE, Hsu SC (2001) The exocyst complex associates with microtubules to mediate vesicle targeting and neurite outgrowth. *J Neurosci* **21:** 3839–3848

Wang KL, Roufogalis BD (1999) Ca2 + /calmodulin stimulates GTP binding to the ras-related protein ral-A. *J Biol Chem* **274:** 14525–14528

Wang L, Li G, Sugita S (2004) RalA-exocyst interaction mediates GTP-dependent exocytosis. *J Biol Chem* **279:** 19875–19881

Wang Q, Navarro MV, Peng G, Molinelli E, Goh SL, Judson BL, Rajashankar KR, Sondermann H (2009) Molecular mechanism of membrane constriction and tubulation mediated by the F-BAR protein Pacsin/Syndapin. *Proc Natl Acad Sci USA* **106:** 12700–12705

Wolthuis RM, Bos JL (1999) Ras caught in another affair: the exchange factors for Ral. *Curr Opin Genet Dev* **9:** 112–117

Wolthuis RM, Zwartkruis F, Moen TC, Bos JL (1998) Ras-dependent activation of the small GTPase Ral. *Curr Biol* **8:** 471–474

Wu H, Rossi G, Brennwald P (2008) The ghost in the machine: small GTPases as spatial regulators of exocytosis. *Trends Cell Biol* **18:** 397–404

Wu S, Mehta SQ, Pichaud F, Bellen HJ, Quiocho FA (2005) Sec15 interacts with Rab11 via a novel domain and affects Rab11 localization *in vivo*. *Nat Struct Mol Biol* **12:** 879–885

Xia Z, Dudek H, Miranti CK, Greenberg ME (1996) Calcium influx *via* the NMDA receptor induces immediate early gene transcription by a MAP kinase/ERK-dependent mechanism. *J Neurosci* **16:** 5425–5436

Zhang J, Schulze KL, Hiesinger PR, Suyama K, Wang S, Fish M, Acar M, Hoskins RA, Bellen HJ, Scott MP (2007a) Thirty-one flavors of Drosophila rab proteins. *Genetics* **176:** 1307–1322

Zhang X, Bi E, Novick P, Du L, Kozminski KG, Lipschutz JH, Guo W (2001) Cdc42 interacts with the exocyst and regulates polarized secretion. *J Biol Chem* **276:** 46745–46750

Zhang X, Orlando K, He B, Xi F, Zhang J, Zajac A, Guo W (2008) Membrane association and functional regulation of Sec3 by phospholipids and Cdc42. *J Cell Biol* **180:** 145–158

Zhang Y, Guo H, Kwan H, Wang JW, Kosek J, Lu B (2007b) PAR-1 kinase phosphorylates Dlg and regulates its postsynaptic targeting at the Drosophila neuromuscular junction. *Neuron* **53:** 201–215